Angle Domain Signal Processing-Aided Channel Estimation for Indoor 60-GHz TDD/FDD Massive MIMO Systems

Dian Fan, Feifei Gao, *Senior Member, IEEE*, Gongpu Wang, Zhangdui Zhong, *Senior Member, IEEE*, and Arumugam Nallanathan, *Fellow, IEEE*

***Abstract*— This paper proposes a practical channel estimation for 60-GHz indoor systems with the massive uniform rectangular array at base station. Through antenna array theory, the parameters of each channel path can be decomposed into the angular information and the channel gain information. We first prove that the true direction of arrivals of each uplink path can be extracted via an efficient array signal processing method. Then, the channel gain information could be obtained linearly with small amount of training resources, which significantly reduces the training overhead and the feedback cost. More importantly, the proposed scheme unifies the uplink/downlink channel estimations for both the time duplex division and frequency duplex division systems, making itself particularly suitable for protocol design. Compared with the existing channel estimation algorithms, the newly proposed one does not require any knowledge of channel statistics and can be efficiently deployed by the 2-D fast Fourier transform. Meanwhile, the number of user terminals simultaneously served can be increased from a sophisticatedly designed angle division multiple access scheme. Simulation results are provided to corroborate the proposed studies.**

***Index Terms*— Massive MIMO, angle domain signal processing, DOA estimation, angle division multiple access (ADMA), angle reciprocity.**

I. Introduction

As a candidate radio band for 5G mobile communications, the millimeter-wave in the range of 30–300 GHz has attracted lots of attention [1]–[3]. Specifically, 60GHz spectrum has been proposed for indoor and short-range outdoor environment since its primary propagation paths only include the line-of-sight (LOS) and the first-order reflections [4]–[6]. For 60 GHz mobile communications, it is possible to equip hundreds or thousands antennas at the base station (BS) due to the short wavelength, resulting in a framework called "massive MIMO" [7]. Theoretically, massive MIMO could tremendously increase the capacity and improve the energy-efficiency. Meanwhile, massive MIMO offers the potential to use economic, inexpensive, and low-power components. These advantages make massive MIMO promising for the next generation wireless systems [8]–[10].

However, all the potential gains of massive MIMO systems rely heavily on the accurate channel estimation at BS, which formulates a great challenge for millimeter-wave indoor scenario [11]. For example, conventional orthogonal training (OT) framework [12] requires the number of the training streams to be proportional to the number of the transmit antennas. Hence, downlink training in massive MIMO systems needs extremely large number of OT sequences. This severe overhead as well as the accompanied high calculation complexity and feedback cost may overwhelm the system performance.

For time division duplexing (TDD) massive MIMO systems, downlink channel state information (CSI) could be obtained via the channel reciprocity [13] from uplink channel estimation [14]–[16]. However, in practice the calibration error of the downlink/uplink RF chains [17] may ruin the channel reciprocity. In addition, channel reciprocity has been proven to be robust only for the single-cell scenario [18]. Moreover, channel reciprocity does not hold for frequency division duplexing (FDD) massive MIMO systems [19]–[25].

In order to reduce the effective number of channel parameters, many works exploited the sparse nature of the channel and claimed the low rank properties in the uplink/downlink channel matrices. Basically there are two main approaches to formulate low rank assumption:

1) Eigen-decomposition based scheme [20]–[22] that directly assume the availability of low rank channel covariance matrices of all user terminals (UTs). However, the complexity of eigen-decomposition based channel estimation is extremely high and this method requires large overhead to obtain reliable channel covariance matrices in practice.
2) Compressive sensing (CS) based scheme [23]–[25] that assume limited number of spatial scattering paths between UTs and BS. However, the complexity of CS

Manuscript received November 3, 2016; revised March 12, 2017; accepted March 24, 2017. Date of publication June 28, 2017; date of current version August 18, 2017. This work was supported in part by the National Natural Science Foundation of China under Grant 61571037, Grant U1334202, Grant 61422109, and Grant 61531011, and in part by the Fundamental Research Funds for the Central Universities under Grant 2016JBZ006. The work of A. Nallanathan was supported by the U.K. EPSRC under Grant EP/M016145/1.

D. Fan is with the State Key Laboratory of Rail Traffic Control and Safety, School of Computer and Information Technology, Beijing Jiaotong University, Beijing 100044, China, and also with the Department of Informatics, King's College London, London WC2R 2LS, U.K. (e-mail: fandian@bjtu.edu.cn).

F. Gao is with the State Key Laboratory of Intelligent Technologies and Systems, Department of Automation, Tsinghua University, Beijing 100084, China, and also with the Tsinghua National Laboratory for Information Science and Technology, Beijing 100084, China (e-mail: feifeigao@ieee.org).

G. Wang and Z. Zhong are with the State Key Laboratory of Rail Traffic Control and Safety, School of Computer and Information Technology, Beijing Jiaotong University, Beijing 100044, China (e-mail: gpwang@bjtu.edu.cn; zhdzhong@bjtu.edu.cn).

A. Nallanathan is with the Queen Mary University of London, London E1 4NS, U.K. (e-mail: a.nallanathan@qmul.ac.uk).

Color versions of one or more of the figures in this paper are available online at http://ieeexplore.ieee.org.

Digital Object Identifier 10.1109/JSAC.2017.2720938

method is still high due to the non-linear optimization while its effectiveness depends on the restricted isometry property (RIP).

In this paper, we propose a practical yet simple channel estimation scheme for 60 GHz indoor communications that could better explore the inherent structure of array. We first exploit the physical characteristics of the massive uniform rectangular array (URA) and decompose the channel information into angular information and gain information. We design an array signal processing aided fast direction of arrival (DOA) estimation algorithm that does not possess the ambiguity problem. The remaining channel gain information could be obtained with small amount of training resources, which significantly reduces the training overhead and the feedback cost. More importantly, the angle reciprocity from antenna array theory says that, the direction of depart (DOD) of the downlink channel is the same as the DOA, which could be utilized to facilitate the downlink channel estimation, especially suitable for FDD system. With the angular information, we further design a user scheduling algorithm, named as angle division multiple access (ADMA), that greatly enhance the spectrum efficiency of both the training and data transmission. Compared to the existing channel estimation algorithms, the newly proposed one does not require the knowledge of channel covariances, does not require eigen-value decomposition of huge matrices, and can be efficiently deployed by the linear estimation approaches.

The rest of the paper is organized as follows. In section II, the system model of 60GHz indoor massive MIMO systems and the channel characteristics are described. In section III, we examine the physical characteristics of URA and propose a fast DOA estimation algorithm. The angular information aided channel estimation algorithm of the uplink transmission are presented in section IV. Section V provides the angular information aided channel estimation algorithm for downlink transmission as well as the user scheduling scheme for downlink data transmission. Simulation results are then presented in Section VI and conclusions are drawn in Section VII.

Notations: Small and upper bold-face letters donate column vectors and matrices respectively; the superscripts $(\cdot)^H$, $(\cdot)^T$, $(\cdot)^*$ stand for the conjugate-transpose, transpose, and conjugate of a matrix, respectively; $tr(\mathbf{A})$ donates the trace of $\mathbf{A}$ and $[\mathbf{A}]_{ij}$ is the (i, j)th entry of $\mathbf{A}$; $diag\{\mathbf{a}\}$ denotes a diagonal matrix with the diagonal element constructed from $\mathbf{a}$, while $diag\{\mathbf{A}\}$ denotes a vector whose elements are extracted from the diagonal components of $\mathbf{A}$; $\mathbb{E}\{\cdot\}$ denotes the statistical expectation, and $\|\mathbf{h}\|$ is the Euclidean norm of $\mathbf{h}$.

II. System Model

In this paper, we consider an indoor environment system with one BS and K single-antenna UTs, as shown in Fig. 1.

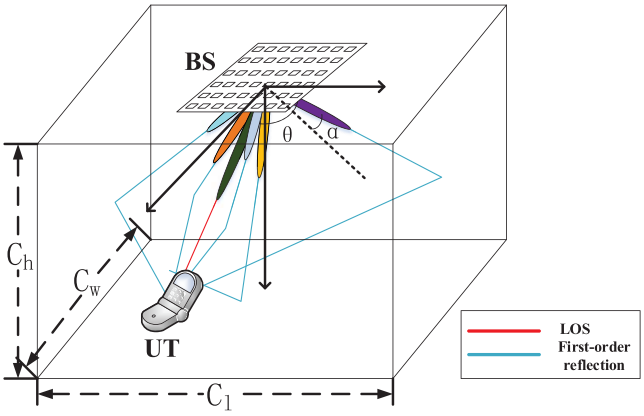

Fig. 1. Indoor environment model showing LOS, first-order reflection propagation paths from a UT element to the BS antenna array.

BS is equipped with $M \times N$ antenna array in the form of URA and is located in the center of ceiling, facing downward. UTs are randomly and uniformly distributed inside room.

Following the measurement results, a statistical model of the meeting-room environment was built in [26], which shows that the line of sight (LOS) path and the 5 first-order reflected paths contribute to the majority of the multipath components, as shown in Fig. 1. Define $\theta_{l,k} \in (-180°, 180°)$ and $\alpha_{l,k} \in (-90°, 90°)$ as the signal azimuth angle and the elevation angle of the lth ($l \leq 6$) path of the kth UT. The corresponding uplink steering matrix [27] can be expressed as (1) shown on bottom of this page, where d denotes the distance between two neighboring elements, and λ is the wave length of the carrier signal. Then the $M \times N$ uplink channel matrix of the lth path of the kth UT can be expressed as

$$\mathbf{H}_{l,k} = a_{l,k}\mathbf{A}(\alpha_{l,k}, \theta_{l,k}), \tag{2}$$

where $a_{l,k} \sim \mathcal{CN}(0, 1)$ denotes the corresponding channel attenuation of the kth UT along path l. Therefore, the overall uplink channel matrix of the kth UT is

$$\mathbf{H}_k = \sum_{l=1}^{6} a_{l,k}\mathbf{A}(\alpha_{l,k}, \theta_{l,k}). \tag{3}$$

Obviously, (3) is a sparse channel model that represents the low rank property and the spatial correlation characteristics of millimeter-wave communications [2], [28], [29]. Nevertheless, our next discussions start from the antenna array theory and will provide different insight from either the eigen-decomposition based scheme [20]–[22] or the CS based scheme [23]–[25]. From (3), it is known that instead of directly estimating the channel $\mathbf{H}_k$, one could separately estimate the DOA information $(\alpha_{l,k}, \theta_{l,k})$, say from angle domain signal processing techniques, and then estimate the

$$\mathbf{A}(\alpha_{l,k}, \theta_{l,k}) = \frac{1}{\sqrt{MN}} \begin{bmatrix} 1 & \cdots & e^{j\frac{2\pi d}{\lambda}(N-1)\sin\alpha_{l,k}\sin\theta_{l,k}} \\ \vdots & \ddots & \vdots \\ e^{j\frac{2\pi d}{\lambda}(M-1)\sin\alpha_{l,k}\cos\theta_{l,k}} & \cdots & e^{j\frac{2\pi d}{\lambda}((M-1)\sin\alpha_{l,k}\cos\theta_{l,k}+(N-1)\sin\alpha_{l,k}\sin\theta_{l,k})} \end{bmatrix}, \tag{1}$$

corresponding path gain $a_{l,k}$. By doing this, the number of the parameters to be treated is greatly reduced. We then define $\mathcal{B}_k = \{(\alpha_{l,k}, \theta_{l,k}), l = 1, 2, \cdots, 6\}$ as the *angular signature* of the kth UT that could uniquely identify a UT inside the indoor environment.

III. DOA Estimation With Antenna Array Theory

In this section, we show how to estimate DOA information from a given $\mathbf{H}_k$, while the detailed channel estimation algorithm to obtain initial $\mathbf{H}_k$ of multiple UTs will be presented in the next section. Conventional DOA estimation, e.g., multiple signal classification (MUSIC) [30] and estimation of signal parameters via rotational invariance technique (ESPRIT) [31]–[34] can be applied for blind DOA estimation. However, these subspace based methods perform eigen-decomposition whose complexity is forbidden for massive MIMO system [35]. Nevertheless, thanks to the massive number of antennas as well as the URA structures, we will demonstrate that the efficient two-dimension fast Fourier transform (2D-FFT) approach can be applied to help DOA estimation.

A. Fast Initial DOA Estimation via 2D-DFT

Define the 2D-DFT of the channel matrix $\mathbf{H}_k$ as $\tilde{\mathbf{H}}_k = \mathbf{F}_M \mathbf{H}_k \mathbf{F}_N$, where $\mathbf{F}_M$ and $\mathbf{F}_N$ are the two normalized DFT matrices, whose (p, q)th elements are $[\mathbf{F}_M]_{pq} = e^{-j\frac{2\pi}{M}pq}/\sqrt{M}$ and $[\mathbf{F}_N]_{pq} = e^{-j\frac{2\pi}{N}pq}/\sqrt{N}$, respectively.

Lemma 1: Most power of $\tilde{\mathbf{H}}_{l,k}$ concentrates around $(i_{l,k}, j_{l,k})$, where $i_{l,k} = \lfloor Md/\lambda \sin\alpha_{l,k}\cos\theta_{l,k} \rceil$, $j_{l,k} = \lfloor Nd/\lambda \sin\alpha_{l,k}\sin\theta_{l,k} \rceil$. Specifically, $\tilde{\mathbf{H}}_{l,k}$ only has one nonzero point $(i_{l,k}, j_{l,k})$ as $M \to \infty, N \to \infty$.

Proof: The (i, j)th component of channel matrix $\tilde{\mathbf{H}}_{l,k}$ is computed as (4).

It can be readily checked that the entries of $\tilde{\mathbf{H}}_{l,k}$ possess sparse property. For example, if $Md/\lambda \sin\alpha_{l,k}\cos\theta_{l,k}$ equals to some integer $i_{l,k}$ and $Nd/\lambda \sin\alpha_{l,k}\sin\theta_{l,k}$ equals to some integer $j_{l,k}$, then $\tilde{\mathbf{H}}_{l,k}$ has only one non-zero element $[\tilde{\mathbf{H}}_{l,k}]_{i_{l,k}, j_{l,k}} = \sqrt{MN}a_{l,k}$, which means that all powers are concentrated on the point $(i_{l,k}, j_{l,k})$. However, for most other cases, $Md/\lambda \sin\alpha_{l,k}\cos\theta_{l,k}$ and $Nd/\lambda \sin\alpha_{l,k}\sin\theta_{l,k}$ are not integers, while the channel power will leak from the point $(\lfloor Md/\lambda \sin\alpha_{l,k}\cos\theta_{l,k} \rceil, \lfloor Nd/\lambda \sin\alpha_{l,k}\sin\theta_{l,k} \rceil)$ (defined as 'central point') to others. In fact, (4) is composed of Sinc function such that the leakage of channel power is inversely proportional to M and N. Hence when M and N are sufficiently large, $\tilde{\mathbf{H}}_{l,k}$ is still a sparse matrix with most of power concentrated around $(Md/\lambda \sin\alpha_{l,k}\cos\theta_{l,k}, Nd/\lambda \sin\alpha_{l,k}\sin\theta_{l,k})$.

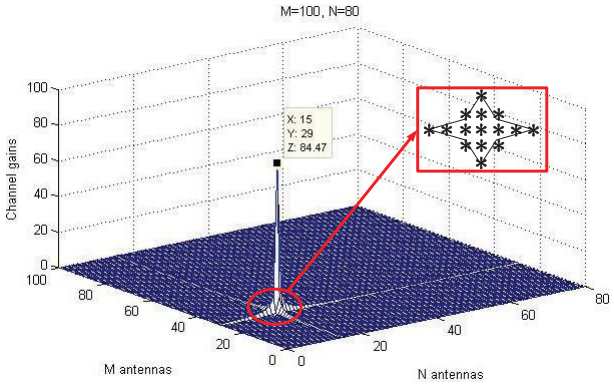

Fig. 2. An example of 2D-DFT sparse characteristics, where BS array has 100×80 antennas.

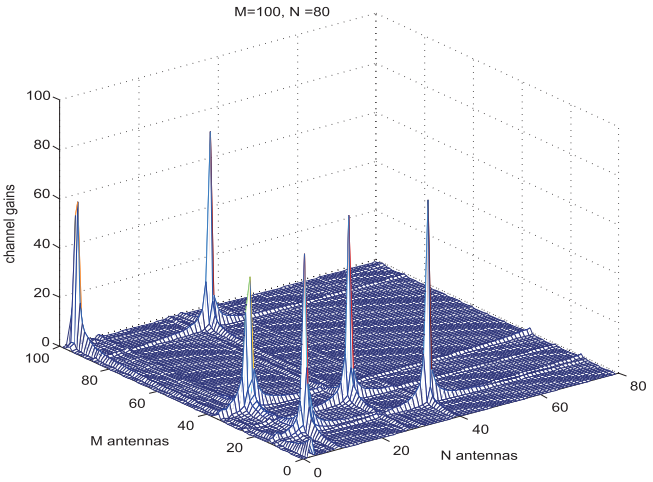

Fig. 3. An example of 2D-DFT sparse characteristics, where BS array has 100×80 antennas.

An example of a single path channel from $(45°, 32°)$ is illustrated in Fig. 2, whose 2D-DFT is depicted. The number of antennas at BS is 100×80. It can be checked that the central point of the channel after 2D-DFT is $(29, 15)$. Moreover, $\eta = 95\%$ channel power concentrates on 15 2D-DFT points as shown in the small planar graph inside Fig. 2.

When $M, N \to \infty$, there always exists integers $(i_{l,k}, j_{l,k})$ that satisfy $Md/\lambda \sin\alpha_{l,k}\cos\theta_{l,k} = i_{l,k}$, $Nd/\lambda \sin\alpha_{l,k}\sin\theta_{l,k} = j_{l,k}$ and all channel powers will concentrate on a single 2D-DFT point $(i_{l,k}, j_{l,k})$, formulating the ideal sparsity. ■

An example of $\tilde{\mathbf{H}}_k$ with $M = 100$ and $N = 80$ is shown in Fig. 3. Hence, the angular signature of the kth user can be immediately obtained from the power-concentrated position in the 2D-DFT of $\mathbf{H}_k$.

$$
\begin{aligned}
[\tilde{\mathbf{H}}_{l,k}]_{i,j} &= \frac{1}{\sqrt{MN}} a_{l,k} \sum_{n=0}^{N-1}\sum_{m=0}^{M-1} e^{-\mathrm{j}(\frac{2\pi}{N}nj + \frac{2\pi}{M}im - 2\pi d/\lambda (m \sin\alpha_{l,k}\cos\theta_{l,k} + n \sin\alpha_{l,k}\sin\theta_{l,k}))} \\
&= \frac{1}{\sqrt{MN}} a_{l,k} e^{-\mathrm{j}\frac{M-1}{2}(\frac{2\pi}{M}i - 2\pi d/\lambda \sin\alpha_{l,k}\cos\theta_{l,k})} e^{-\mathrm{j}\frac{N-1}{2}(\frac{2\pi}{N}j - 2\pi d/\lambda \sin\alpha_{l,k}\sin\theta_{l,k})} \\
&\quad \cdot \frac{\sin[\frac{M}{2}(\frac{2\pi}{M}i - 2\pi d/\lambda \sin\alpha_{l,k}\cos\theta_{l,k})]}{\sin[\frac{1}{2}(\frac{2\pi}{M}i - 2\pi d/\lambda \sin\alpha_{l,k}\cos\theta_{l,k})]} \cdot \frac{\sin[\frac{N}{2}(\frac{2\pi}{N}j - 2\pi d/\lambda \sin\alpha_{l,k}\sin\theta_{l,k})]}{\sin[\frac{1}{2}(\frac{2\pi}{N}j - 2\pi d/\lambda \sin\alpha_{l,k}\sin\theta_{l,k})]}.
\end{aligned} \tag{4}
$$

Remark 1: Since there only exist 6 paths from one UT to BS, the power of the equivalent channel matrix $\tilde{\mathbf{H}}_k$ will concentrate around 6 bins, and is thus sparse. Hence, the eigen-decomposition based scheme [20]–[22] and the CS-based scheme [23]–[25] also proposed to estimate the limited parameters in $\tilde{\mathbf{H}}_k$ if one estimate $\tilde{\mathbf{H}}_k$ instead of $\mathbf{H}_k$. However, the eigen-decomposition based method require the $M \times N$ dimensional channel covariance matrix, while the CS-based method, will have to handle much more non-zero entries in $\tilde{\mathbf{H}}_k$ due to the power leakage problem. Nevertheless, we next show that the power leakage problem can be removed with the aid of array signal processing approach, and the exact DOA estimation can be obtained.

B. Fine DOA Estimation via Angular Rotation

Lemma 2: Define

$$\begin{aligned}\Phi_M(\Delta\alpha_{l,k}) &= diag(1, e^{j\Delta\alpha_{l,k}}, \cdots, e^{j(M-1)\Delta\alpha_{l,k}}),\\ \Phi_N(\Delta\theta_{l,k}) &= diag(1, e^{j\Delta\theta_{l,k}}, \cdots, e^{j(N-1)\Delta\theta_{l,k}}),\end{aligned} \tag{5}$$

where $\Delta\alpha_{l,k} \in [-\frac{\pi}{M}, \frac{\pi}{M}]$ and $\Delta\theta_{l,k} \in [-\frac{\pi}{N}, \frac{\pi}{N}]$ are the phase rotation parameters. The angular rotation *operation $\tilde{\mathbf{H}}^{ro}_{l,k} = \mathbf{F}_M\Phi_M(\Delta\alpha_{l,k})\mathbf{H}_{l,k}\Phi_N(\Delta\theta_{l,k})\mathbf{F}_N$ can concentrate all power within one entry of $\tilde{\mathbf{H}}^{ro}_{l,k}$ when*

$$\begin{aligned}\Delta\alpha_{l,k} &= (2\pi/Mi_{l,k} - 2\pi d/\lambda \sin\alpha_{l,k}\cos\theta_{l,k}) \in [-\pi/M, \pi/M],\\ \Delta\theta_{l,k} &= (2\pi/Nj_{l,k} - 2\pi d/\lambda \sin\alpha_{l,k}\sin\theta_{l,k}) \in [-\pi/N, \pi/N].\end{aligned} \tag{6}$$

Proof: The (i, j)th element of $\tilde{\mathbf{H}}^{ro}_{l,k}$ can be calculated as (7). It can be readily checked that the entries of $\tilde{\mathbf{H}}^{ro}_{l,k}$ has only one non-zero element $[\tilde{\mathbf{H}}_{l,k}]^{ro}_{i_{l,k}, j_{l,k}} = \sqrt{MN}a_{l,k}$. ■

Lemma 2 indicates that: when we gradually rotate $\mathbf{H}_k$ by $\Delta\alpha \in [-\frac{\pi}{M}, \frac{\pi}{M}]$ and $\Delta\theta \in [-\frac{\pi}{N}, \frac{\pi}{N}]$, then the original 6 bins in 2D-DFT domain will shrink to a single sharp peak one by one (not simultaneously). Then, the corresponding rotation value $(\Delta\alpha, \Delta\theta)$ would serve as a good estimate of $(\Delta\alpha_{l,k}, \Delta\theta_{l,k})$ in Lemma 2. Together with the previously obtained coarse DOA estimation from 2D-DFT, we could get a fine DOA estimation as:

$$\begin{aligned}\hat{\alpha}_{l,k} &= \arcsin\left(\lambda/d\sqrt{\left(\frac{i_{l,k}}{M} - \frac{\Delta\alpha_{l,k}}{2\pi}\right)^2 + \left(\frac{j_{l,k}}{N} - \frac{\Delta\theta_{l,k}}{2\pi}\right)^2}\right),\\ \hat{\theta}_{l,k} &= \arctan\frac{\frac{j_{l,k}}{N} - \frac{\Delta\theta_{l,k}}{2\pi}}{\frac{i_{l,k}}{M} - \frac{\Delta\alpha_{l,k}}{2\pi}}.\end{aligned} \tag{8}$$

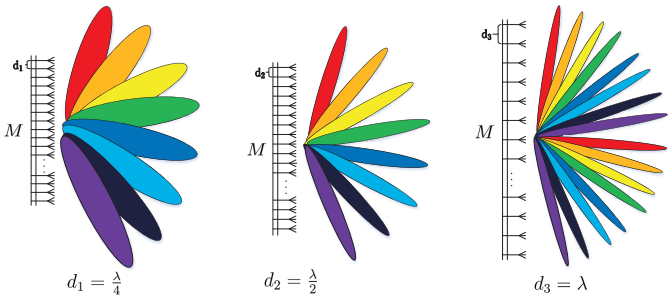

Fig. 4. The spatial resolution of different antenna spacing $d_1 = \frac{\lambda}{4}$, $d_2 = \frac{\lambda}{2}$, $d_3 = \lambda$, respectively, with a constant number of antennas M.

Remark 2: Though quite a few beamspace works [36]–[38] claim that the 2D-DFT of channels could already represent the angle information of the UTs, it is known from section III.A that such direct 2D-DFT of channels could merely presents the angle information "on the discrete grids" but is not the true angle information of the UTs when practical array is of finite size. As will be seen later, utilizing the true angle information of the channel, named angle domain, *can offer many benefits, for example, the less power leakage and the simplified downlink channel estimation due to angle reciprocity.*

C. Spatial Resolution and DOA Ambiguity

Though antenna array theory does help to decouple the channel estimation of $\mathbf{H}_k$ into DOA estimation and gain estimation which then reduces the number of the parameters to be estimated, it meanwhile brings some inherent problem during DOA estimation. For example, the spatial resolution and DOA ambiguity that is related to the aperture of antenna array should be carefully handled.

It is well known that the resolution of DOA estimation can be improved by enlarging the antenna spacing without changing the number of antennas. It can be seen from Fig. 4 that when the antenna spacing increases (up to $\lambda/2$), the width

$$\begin{aligned}[\tilde{\mathbf{H}}^{ro}_{l,k}]_{i,j} &= [\mathbf{F}_M\Phi_M(\Delta\alpha_{l,k})\mathbf{H}_{l,k}\Phi_N(\Delta\theta_{l,k})\mathbf{F}_N]_{i,j}\\ &= \frac{1}{\sqrt{MN}}a_{l,k}\sum_{n=0}^{N-1}\sum_{m=0}^{M-1} e^{-j(\frac{2\pi}{N}nj + \frac{2\pi}{M}im - 2\pi d/\lambda(m\sin\alpha_{l,k}\cos\theta_{l,k} + n\sin\alpha_{l,k}\sin\theta_{l,k}) - m\Delta\alpha_{l,k} - n\Delta\theta_{l,k})}\\ &= \frac{1}{\sqrt{MN}}a_{l,k}e^{-j\frac{M-1}{2}(\frac{2\pi}{M}i - 2\pi d/\lambda\sin\alpha_{l,k}\cos\theta_{l,k} - \Delta\alpha_{l,k})}e^{-j\frac{N-1}{2}(\frac{2\pi}{N}j - 2\pi d/\lambda\sin\alpha_{l,k}\sin\theta_{l,k} - \Delta\theta_{l,k})}\\ &\quad\cdot\frac{\sin[\frac{M}{2}(\frac{2\pi}{M}i - 2\pi d/\lambda\sin\alpha_{l,k}\cos\theta_{l,k} - \Delta\alpha_{l,k})]}{\sin[\frac{1}{2}(\frac{2\pi}{M}i - 2\pi d/\lambda\sin\alpha_{l,k}\cos\theta_{l,k} - \Delta\alpha_{l,k})]}\cdot\frac{\sin[\frac{N}{2}(\frac{2\pi}{N}j - 2\pi d/\lambda\sin\alpha_{l,k}\sin\theta_{l,k} - \Delta\theta_{l,k})]}{\sin[\frac{1}{2}(\frac{2\pi}{N}j - 2\pi d/\lambda\sin\alpha_{l,k}\sin\theta_{l,k} - \Delta\theta_{l,k})]}.\\ &= \frac{1}{\sqrt{MN}}a_{l,k}e^{-j\frac{(M-1)\pi}{M}(i-i_{l,k})}e^{-j\frac{(N-1)\pi}{N}(j-j_{l,k})}\cdot\frac{\sin[\pi(i-i_{l,k})]}{\sin[\frac{\pi}{M}(i-i_{l,k})]}\cdot\frac{\sin[\pi(j-j_{l,k})]}{\sin[\frac{\pi}{N}(j-j_{l,k})]}.\end{aligned} \tag{7}$$

of beam becomes smaller while the number of the orthogonal beams that the antenna could formulate keeps as M. When the antennas spacing keeps on increasing (above $\lambda/2$), the width of beam continues to shrink while there start appearing the ambiguous beams, namely, the same steering vector corresponds to two beams in the space. Therefore, the antenna spacing of URA should generally be restricted to no larger than $\lambda/2$ to avoid the DOA ambiguity. For indoor communications, the situation of DOA estimation would be a bit different. For example, the height of the UT is limited by the height of human being and thus UTs would not be distributed over all 3D space inside the room. In this case, the elevation angle α and azimuth angle θ may stay in a smaller range than $(-\pi, \pi)$, say $\alpha \in (\alpha_{min}, \alpha_{max})$, $\theta \in (\theta_{min}, \theta_{max})$. It is then possible to increase the antenna spacing to be greater than $\lambda/2$ without causing the DOA estimation ambiguity.

Let us assume the length, the width and the height of the indoor cuboid as C_l, C_w, C_h respectively, as shown in Fig. 1. Moreover, assume the maximum height of the UT is C_m. The maximum angle of elevation arise when UT is located in the edge of the room. We can obtain

$$\tan\alpha_{max} = \frac{\sqrt{(\frac{3}{2}C_l)^2 + (\frac{1}{2}C_w)^2}}{C_h - C_m} = \frac{\sqrt{C_w^2 + 9C_l^2}}{2(C_h - C_m)}. \quad (9)$$

Thus, α_{max} can be expressed as

$$\alpha_{max} = \arctan\left(\frac{\sqrt{C_w^2 + 9C_l^2}}{2(C_h - C_m)}\right). \quad (10)$$

If UTs are randomly distributed on the ground, then the coverage of BS is limited within $\theta_{l,k} \in [-\pi, \pi]$ and $\alpha_{l,k} \in [-\alpha_{max}, \alpha_{max}]$. The DOA ambiguity happens if there exist pseudo DoAs $\tilde{\alpha}$, $\tilde{\theta}$ and satisfy

$$\begin{aligned} 2\pi\frac{d_1}{\lambda}(\sin\alpha\cos\theta - \sin\tilde{\alpha}\cos\tilde{\theta}) &= 2k\pi, k = 0, \pm1, \ldots, \\ 2\pi\frac{d_2}{\lambda}(\sin\alpha\sin\theta - \sin\tilde{\alpha}\sin\tilde{\theta}) &= 2k\pi, k = 0, \pm1, \ldots. \end{aligned} \quad (11)$$

To avoid DOA ambiguity, there should be no solutions to (11) for $\tilde{\alpha} \in [-\alpha_{max}, \alpha_{max}]$ and $\tilde{\theta} \in [-\pi, \pi]$. Thus we obtain

$$\begin{aligned} \sin\alpha\cos\theta - \frac{\lambda}{d_1} &\le (\sin\tilde{\alpha}\cos\tilde{\theta})_{min}, \\ \sin\alpha\cos\theta + \frac{\lambda}{d_1} &\ge (\sin\tilde{\alpha}\cos\tilde{\theta})_{max}, \\ \sin\alpha\sin\theta - \frac{\lambda}{d_2} &\le (\sin\tilde{\alpha}\sin\tilde{\theta})_{min}, \\ \sin\alpha\sin\theta + \frac{\lambda}{d_2} &\ge (\sin\tilde{\alpha}\sin\tilde{\theta})_{max}, \end{aligned} \quad (12)$$

which are equivalent to

$$\begin{aligned} \frac{d_1}{\lambda} &\le \frac{1}{\sin\alpha\cos\theta - (\sin\tilde{\alpha}\cos\tilde{\theta})_{min}}, \\ \frac{d_1}{\lambda} &\le \frac{1}{(\sin\tilde{\alpha}\cos\tilde{\theta})_{max} - \sin\alpha\cos\theta}, \\ \frac{d_2}{\lambda} &\le \frac{1}{\sin\alpha\sin\theta - (\sin\tilde{\alpha}\sin\tilde{\theta})_{min}}, \\ \frac{d_2}{\lambda} &\le \frac{1}{(\sin\tilde{\alpha}\sin\tilde{\theta})_{max} - \sin\alpha\sin\theta}, \end{aligned} \quad (13)$$

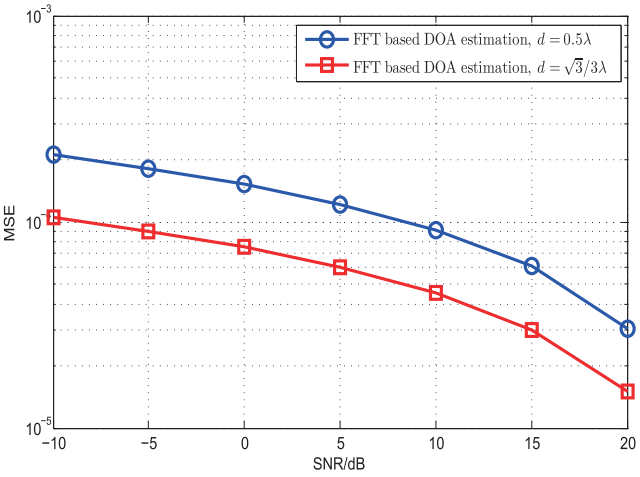

Fig. 5. Comparison of the proposed FFT based DOA estimation method with $d = 0.5\lambda$ and $d = \frac{\sqrt{3}}{3}\lambda$, respectively.

where $(\cdot)_{min}$ and $(\cdot)_{max}$ denote the minimum value and the maximum value of the argument inside when $\tilde{\alpha}$ and $\tilde{\theta}$ go through their respective range.

For example, let us take $C_l = 3, C_w = 2, C_h = 3.5$, and $C_m = 0.5$. Then, $\alpha_{max} = \arctan\frac{\sqrt{85}}{6} \approx \frac{2\pi}{3}$. From (13), we can obtain the following inequalities

$$\begin{aligned} \frac{d_1}{\lambda} &\le \frac{1}{|\sin\alpha\cos\theta + \frac{\sqrt{3}}{2}|}, \frac{d_1}{\lambda} \le \frac{1}{|\frac{\sqrt{3}}{2} - \sin\alpha\cos\theta|}, \\ \frac{d_2}{\lambda} &\le \frac{1}{|\sin\alpha\sin\theta + \frac{\sqrt{3}}{2}|}, \frac{d_2}{\lambda} \le \frac{1}{|\frac{\sqrt{3}}{2} - \sin\alpha\sin\theta|}. \end{aligned} \quad (14)$$

Hence, we can obtain $d_1 \le \frac{\sqrt{3}}{3}\lambda$ and $d_2 \le \frac{\sqrt{3}}{3}\lambda$, which are greater than $\lambda/2$. In this case, one should set the array aperture exactly as $d_1 = \frac{\sqrt{3}}{3}\lambda$ and $d_2 = \frac{\sqrt{3}}{3}\lambda$ to enhance the accuracy of DOA estimation.

To verify that the larger antenna aperture does increase the DOA estimation accuracy, we demonstrate the DOA estimation results of the proposed algorithm in Fig. 5 with $M = 100, N = 100$ for different antenna spacing d. The number of UTs is taken only as 1 for illustration. The mean square error (MSE) of the DOAs are defined as

$$\text{MSE} = \sum_{l=1}^{6}\left(\frac{|\hat{\alpha}_l - \alpha_l|^2}{\alpha_l^2} + \frac{|\hat{\theta}_l - \theta_l|^2}{\theta_l^2}\right)\Big/6. \quad (15)$$

It is seen that when antenna spacing d increases, the MSE of the proposed FFT algorithm reduces while there is no DOA estimation ambiguity.

IV. Uplink Channel Estimation Strategy

In this section, we propose a communication framework that include uplink preamble, uplink training, uplink data transmission, downlink training, and downlink data transmission, as shown in Fig. 6. The transmission initializes from an uplink preamble to obtain the angular signature of all UTs with the aid of the algorithm in the previous section. Then UTs are grouped and scheduled for the subsequent uplink/downlink training and

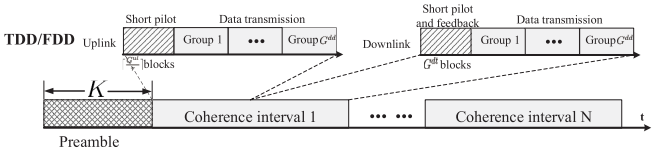

Fig. 6. A unified transmission scheme including preamble, uplink/downlink training and data transmission.

data transmission based on their respective angular signature. It needs to be mentioned that the proposed framework is applicable for both TDD and FDD schemes.

A. Obtain Angular Signature Through Uplink Preamble

During the preamble stage, each UT send the orthogonal training sequence to obtain their initial channel estimate. If the number of available orthogonal training sequences is limited, say smaller than the number of users, then each UT would have to sequentially reuse orthogonal training sequences. To ease illustration, we assume K orthogonal training sequences are available at preamble stage and the length of the training sequences is also equal to K. This process seems time consuming but will only be performed once at the start of the transmission, as will be explained later.

Denote the available orthogonal training sequences set as $\mathbf{P} = [\mathbf{p}_1, \mathbf{p}_2, \cdots, \mathbf{p}_K]$ with $\mathbf{p}_i^H \mathbf{p}_j = K \cdot \sigma_p^2 \cdot \delta(i-j)$ and σ_p^2 being the average training power. The tensor of the received training signals $\mathcal{Y} \in \mathbb{C}^{M\times N\times K}$ at BS can be written as

$$\mathcal{Y} = \sum_{k=1}^{K} (\mathcal{H}_k \times_3 \mathbf{p}_k + \mathcal{N}_k), \tag{16}$$

where $\mathcal{H}_k \in \mathbb{C}^{M\times N\times 1}$ is the uplink channel tensor[1] [39] for the kth UT, $[\mathcal{H}_k]_{:,:,1} = \mathbf{H}_k$, and $\mathcal{N}_k \in \mathbb{C}^{M\times N\times K}$ is the independent additive white Gaussian noise tensor with elements distributed as $\mathcal{CN}(0,1)$. Since the first two dimensions of $\mathcal{H}_k$ denote the BS antennas and the third dimension represents UT antenna, we may use $\times_3$ to obtain the received signal $\mathcal{Y}$. Hence, the least square (LS) estimation of the channel $\mathcal{H}_k$ can be expressed as

$$\begin{aligned}\widehat{\mathcal{H}_k} &= \frac{1}{K\sigma_p^2}\mathcal{Y} \times_3 \mathbf{p}_k^H = \frac{1}{K\sigma_p^2}\sum_{k'=1}^{K} (\mathcal{H}_{k'} \times_3 \mathbf{p}_{k'} + \mathcal{N}_{k'}) \times_3 \mathbf{p}_k^H \\ &= \mathcal{H}_k + \frac{1}{K\sigma_p^2}\mathcal{N}_k \times_3 \mathbf{p}_k^H = \mathcal{H}_k + \frac{1}{\sqrt{K(\frac{\sigma_p^2}{\sigma_n^2})}}\mathcal{N}_k, \end{aligned} \tag{17}$$

where σ_p^2/σ_n^2 is defined as the uplink training signal-to-noise ratio (SNR), and $\mathcal{N}_k$ denotes the normalized Gaussian white noise.

Repeating the similar operations in (17) for all G groups yields the channel estimates for all K UTs. The next step is to obtain 6 angular rotations $(\Delta\alpha_{l,k}, \Delta\theta_{l,k}), l = 1, 2, \cdots, 6$ and extract the angular signature $\mathcal{B}_k = \{(\alpha_{l,k}, \theta_{l,k}), l = 1, 2, \cdots, 6\}$ of each UT via the 2D-DFT and angular rotation approaches in previous section. The detailed steps are summarized in Algorithm 1:

[1]In this paper, we consider the three-dimensional tensor whose element is (x, y, z). The corresponding algebra of tensors is provided in the appendix.

Algorithm 1 Obtaining the angular signature from uplink preamble

Step 1: Extract the estimation of $\hat{\mathbf{H}}_k$ as $\hat{\mathbf{H}}_k = [\hat{\mathcal{H}}_k]_{:,:,1}$ for all UTs. After 2D-DFT of $\hat{\mathbf{H}}_k$, we can obtain $\tilde{\hat{\mathbf{H}}}_k = \mathbf{F}_M \hat{\mathbf{H}}_k \mathbf{F}_N$, which have 6 original bins $\mathcal{F}_{l,k}, l = 1, 2, \cdots, 6$, as shown in Fig. 3.

Step 2: *Initial estimation via 2D-DFT*: Select the element with the maximal power in each original bins, respectively. Namely, $Q_{l,k} = \text{argmax}_{(i,j)\in\mathcal{F}_{l,k}} \|[\tilde{\hat{\mathbf{H}}}_k]_{i,j}\|^2$, and the location of the maximal power $Q_{l,k}$ in lth original bin is $(i_{l,k}, j_{l,k}) = (i, j)$.

Step 3: *Fine estimation via angular rotation*: Search for $\Delta\alpha \in [-\frac{\pi}{M}, \frac{\pi}{M}]$ and $\Delta\theta \in [-\frac{\pi}{N}, \frac{\pi}{N}]$ with a certain precision, and define $\tilde{\hat{\mathbf{H}}}_k^{ro} = \mathbf{F}_M \Phi_M(\Delta\alpha) \hat{\mathbf{H}}_k \Phi_N(\Delta\theta) \mathbf{F}_N$, which also have 6 bins. For each original bins $\mathcal{F}_{l,k}$, if $\text{argmax}_{(i,j)\in\mathcal{F}_{l,k}} \|[\tilde{\hat{\mathbf{H}}}_k^{ro}]_{i,j}\|^2 > Q_{l,k}$, we update $Q_{l,k} = \text{argmax}_{(i,j)\in\mathcal{F}_{l,k}} \|[\tilde{\hat{\mathbf{H}}}_k^{ro}]_{i,j}\|^2$, $\Delta\alpha_{l,k} = \Delta\alpha, \Delta\theta_{l,k} = \Delta\theta$, $(i_{l,k}, j_{l,k}) = (i, j)$.

Step 4: After searching all $\Delta\alpha$ and $\Delta\theta$, we can obtain the location of the maximal power $Q_{l,k}$ and the optimal angular rotation $(\Delta\alpha_{l,k}, \Delta\theta_{l,k})$ for each bin of all UTs.

Step 5:The angular information $(\hat{\alpha}_{l,k}, \hat{\theta}_{l,k})$ can be estimated from (8). After that, the angular signature $\mathcal{B}_k = \{(\hat{\alpha}_{l,k}, \hat{\theta}_{l,k}), l = 1, 2, \cdots, 6\}$ of the kth UT can be obtained.

The number of search grids within $[-\frac{\pi}{M}, \frac{\pi}{M}]$ and $[-\frac{\pi}{N}, \frac{\pi}{N}]$ determines the accuracy and the complexity of the whole algorithm. We denote G as the search grids, which are evenly distributed in $[-\frac{\pi}{M}, \frac{\pi}{M}]$ and $[-\frac{\pi}{N}, \frac{\pi}{N}]$. Clearly, the number of search grids is inversely proportional to the complexity of the algorithm but is proportional to the accuracy of the algorithm. Then we can obtain the complexity of the worst MSE is about $O(MN \log MN + MN + GKMN)$, which is much smaller than $O((MN)^3)$ especially when M, N is large. In fact, for massive MIMO with very large M, N, a small value of G is already good enough to provide very high accuracy and low complexity.

B. Channel Estimation With ADMA

The preamble will only be sent once at the beginning of the transmission. Afterwards, the CSI should be re-estimated when it exceeds the coherent time. Nevertheless, since a UT may not physically change its position in a relatively longer time, we may treat the DOA component of the channel as unchanged within several or even tens of the channel coherence times, while the remaining gain component could be re-estimated via much simplified approach. After preamble, we assume that there are only $\tau < K$ short pilot sequences with length $L(\tau \le L)$ in uplink training stage. Specifically, with the angular information obtained from preamble, UTs can be grouped and served simultaneously.

Let us divide K UTs into G^{ul} groups while UTs in each group satisfy $\mathcal{B}_{k_1} \cap \mathcal{B}_{k_2} = \emptyset, k_1 \neq k_2$ and $\mathcal{B}_{k_1} - \mathcal{B}_{k_2} \ge \mathbf{\Omega}$, where $\mathbf{\Omega}$ denotes the guard interval and $\mathcal{B}_{k_1} - \mathcal{B}_{k_2}$ means the minimum distance of the elements in $\mathcal{B}_{k_1}$ and $\mathcal{B}_{k_2}$. Namely,

$(\alpha_{l,k_1} - \alpha_{l,k_2})_{min} \geq \Omega$ and $(\theta_{l,k_1} - \theta_{l,k_2})_{min} \geq \Omega$. Since each $\mathcal{B}_k$ contains only 6 path, one group could easily contain multiple UTs and then $G^{\text{ul}} \ll K$ generally holds. Since UTs are grouped based on their angular information, we name this scheme as ADMA. For the ease of illustration, let us assume $G^{\text{ul}} \leq \tau$. Moreover, denote the UT set of the gth group as $\mathcal{U}_g$.

Let us then assign the training sequence $\mathbf{s}_g$ to the gth group and allow all UTs to transmit the training sequences simultaneously. The received signals at BS can then be expressed as

$$\mathcal{Y} = \sum_{g=1}^{G^{\text{ul}}} \sum_{k \in \mathcal{U}_g} \mathcal{H}_k \times_3 \mathbf{s}_g + \mathcal{N}. \tag{18}$$

Similar to (17), we could obtain

$$\begin{aligned}\widehat{\mathcal{H}}_g &= \frac{1}{L\sigma_s^2}\mathcal{Y} \times_3 \mathbf{s}_g^H = \frac{1}{L\sigma_s^2}\Big(\sum_{g=1}^{G^{\text{ul}}} \sum_{k \in \mathcal{U}_g} \mathcal{H}_k \times_3 \mathbf{s}_g + \mathcal{N}\Big) \times_3 \mathbf{s}_g^H \\ &= \mathcal{H}_k + \sum_{l \in \mathcal{U}_g/\{k\}} \mathcal{H}_l + \frac{1}{L\sigma_s^2}\mathcal{N} \times_3 \mathbf{s}_g^H \\ &= \mathcal{H}_k + \sum_{l \in \mathcal{U}_g/\{k\}} \mathcal{H}_l + \frac{1}{\sqrt{L(\frac{\sigma_s^2}{\sigma_n^2})}}\mathcal{N}_g. \end{aligned} \tag{19}$$

Obviously, the second term in the last equation contains channel matrices of all the other UTs in the same group and is the so called *pilot contamination*.

Lemma 3: For massive MIMO scenario, i.e., $M \to \infty$, $N \to \infty$, the following property holds:

$$\lim_{\substack{M\to\infty \\ N\to\infty}} vec(\mathbf{A}(\alpha_1, \theta_1))^H vec(\mathbf{A}(\alpha_2, \theta_2)) = \begin{cases} \mathbf{1}, & \substack{\alpha_1=\alpha_2 \\ \theta_1=\theta_2} \\ \mathbf{0}, & otherwise. \end{cases} \tag{20}$$

Proof: Define

$$\mathbf{a}(v_{\alpha,\theta}) = \frac{1}{\sqrt{M}}[1, e^{j2\pi\frac{d}{\lambda}\sin\alpha\cos\theta}, \ldots, e^{j2\pi\frac{d}{\lambda}(M-1)\sin\alpha\cos\theta}]^H, \tag{21}$$

$$\mathbf{a}(u_{\alpha,\theta}) = \frac{1}{\sqrt{N}}[1, e^{j2\pi\frac{d}{\lambda}\sin\alpha\sin\theta}, \ldots, e^{j2\pi\frac{d}{\lambda}(M-1)\sin\alpha\sin\theta}]^H. \tag{22}$$

It can be easily checked that $\text{vec}(\mathbf{A}(\alpha_i, \theta_i)) = \mathbf{a}(v_{\alpha_i,\theta_i}) \otimes \mathbf{a}(u_{\alpha_i,\theta_i})$, for $i = 1, 2$. Then there is

$$\begin{aligned}&\lim_{M\to\infty,N\to\infty} \text{vec}(\mathbf{A}(\alpha_1, \theta_1))^H \text{vec}(\mathbf{A}(\alpha_2, \theta_2)) \\ &= \lim_{M\to\infty,N\to\infty} [\mathbf{a}(v_{\alpha_1,\theta_1}) \otimes \mathbf{a}(u_{\alpha_1,\theta_1})]^H [\mathbf{a}(v_{\alpha_2,\theta_2}) \otimes \mathbf{a}(u_{\alpha_2,\theta_2})] \\ &= \lim_{M\to\infty,N\to\infty} [\mathbf{a}(v_{\alpha_1,\theta_1})^H \mathbf{a}(v_{\alpha_2,\theta_2})] \otimes [\mathbf{a}(u_{\alpha_1,\theta_1})^H \mathbf{a}(u_{\alpha_2,\theta_2})] \\ &= \delta(\sin\alpha_1\cos\theta_1 - \sin\alpha_2\cos\theta_2) \cdot \delta(\sin\alpha_1\sin\theta_1 - \sin\alpha_2\sin\theta_2), \end{aligned} \tag{23}$$

where $\delta(\cdot)$ is the Dirac delta function and the nonzero value is obtained if and only if

$$\begin{cases} \sin\alpha_1\cos\theta_1 = \sin\alpha_2\cos\theta_2 \\ \sin\alpha_1\sin\theta_1 = \sin\alpha_2\sin\theta_2 \end{cases} \overset{(a)}{\Longleftrightarrow} \begin{cases} \alpha_1 = \alpha_2 \\ \theta_1 = \theta_2. \end{cases} \tag{24}$$

and $\overset{(a)}{\Longleftrightarrow}$ is due to the bounded range of $\alpha_1, \alpha_2, \theta_1, \theta_2 \in [0, \pi]$. Therefore, we get that different channels for different angular signature will be orthogonal when M and N approach infinity. ■

Let us then multiply both sides of (19) by steering vector $\text{vec}^H(\mathbf{A}(\hat{\alpha}_{l,k}, \hat{\theta}_{l,k}))$ and obtain

$$\begin{aligned}&\text{vec}^H(\mathbf{A}(\hat{\alpha}_{l,k}, \hat{\theta}_{l,k}))[\widehat{\mathcal{H}}_g]_{(3)} \\ &= \text{vec}^H(\mathbf{A}(\hat{\alpha}_{l,k}, \hat{\theta}_{l,k}))([\mathcal{H}_k]_{(3)} + \sum_{l \in \mathcal{U}_g/\{k\}} [\mathcal{H}_l]_{(3)} \\ &\quad + \frac{1}{\sqrt{L(\frac{\sigma_s^2}{\sigma_n^2})}}[\mathcal{N}_g]_{(3)}) \\ &= a_{l,k} + \frac{1}{\sqrt{L(\frac{\sigma_s^2}{\sigma_n^2})}}\text{vec}^H(\mathbf{A}(\hat{\alpha}_{l,k}, \hat{\theta}_{l,k}))[\mathcal{N}_g]_{(3)}. \end{aligned} \tag{25}$$

According to Lemma. 3 and bearing in mind that $\mathcal{B}_k$ and $\mathcal{B}_l$ are separated at least by one guard interval $\mathbf{\Omega}$, we know the entries of $\sum_{l \in \mathcal{U}_g/\{k\}} \text{vec}^H(\mathbf{A}(\hat{\alpha}_{l,k}, \hat{\theta}_{l,k}))[\mathcal{H}_l]_{(3)}$ in (25) approximate to zero for massive URA. Clearly (25) could serve as good estimate for $a_{l,k}$ and is thus denoted as $\hat{a}_{l,k}$.

With the angular information from (8) and gain information from (25), we may obtain the normalized uplink channel estimation for all UTs as

$$[\hat{\mathcal{H}}_k]_{(3)} = \sum_{l=1}^{6} \hat{a}_{l,k} \text{vec}(\mathbf{A}(\hat{\alpha}_{l,k}, \hat{\theta}_{l,k})). \tag{26}$$

Remark 3: The aforementioned discussions have illuminated the framework for pilot reusing and user scheduling during uplink training, where the same training sequences can be reused if UTs do not have overlapped angular signature, namely, they are "orthogonal in angle domain". While for those UTs that cannot be spatially separated, they have to use "orthogonal training" to avoid the pilot contamination. Moreover, the key 2D-DFT operation in the proposed scheme can be efficiently implemented by 2D-FFT.

V. Downlink Transmission Strategy

A. Downlink Channel Estimation With Angle Reciprocity

The key difficulty to apply the conventional downlink channel estimation algorithms for massive MIMO systems lies in the requirement that the length of the training has to be no less than the number of antennas. Moreover, the feedback of huge CSI from UTs back to BS also costs severe overhead. For TDD systems, the estimated uplink channel can be used as downlink channel by the property of channel reciprocity. However, for FDD systems the channel reciprocity does not hold.

It has been shown in [40]–[43] that the uplink and downlink channel may have similar angular information due to the characteristics of the physical propagation, especially when the uplink and downlink frequencies are not far from each other. Namely, the directional of departure (DOD) of the downlink channel is the same as the DOA of the uplink channel that have been estimated through preamble. This property is then named as *angular reciprocity*. A side proof of angular reciprocity can be found in Table. I [41], showing the values of the relative permittivity, the conductivity, and the frequency range of a

TABLE I
PARAMETERS FOR THE RELATIVE PERMITTIVITY AND CONDUCTIVITY OF BUILDING MATERIALS [41]

Material class	Relative permittivity	Conductivity		Frequency range (GHz)
Concrete	5.31	0.0326	0.8095	1-100
Brick	3.75	0.038	0.0	1-10
Plasterboard	2.94	0.0116	0.7076	1-100
Wood	1.99	0.0047	1.0718	0.001-100
Glass	6.27	0.0043	1.1925	0.1-100
Ceiling board	1.50	0.0005	1.1634	1-100
Chipboard	2.58	0.0217	0.7800	1-100
Floorboard	3.66	0.0044	1.3515	50-100
Metal	1	10^7	0.0	1-100

number of building materials. It is seen that the propagation characteristic may not change for the frequency variation up to 10GHz, theoretically. In practice, the downlink and uplink frequency in 60 GHz could be away for as large as several gigaHertz. In this case, DOA and DOD could be different by a small value, which could nevertheless be compensated for via beaming sweeping method within a small region [44].

Denote the downlink channel from BS to the kth UT as $\mathbf{G}_k$. Similar to (3), $\mathbf{G}_k$ can be modeled as

$$\mathbf{G}_k = \sum_{l=1}^{6} \beta_{l,k} \mathbf{A}(\alpha_{l,k}, \theta_{l,k}), \tag{27}$$

where $\mathbf{A}(\alpha_{l,k}, \theta_{l,k})$ is the steering matrix defined in (1) but with different downlink carrier wavelength λ, and $\beta_{l,k}$ is the corresponding downlink channel gain of each path that is to be estimated. All other parameters have the same definitions as in (3).

Denote $\mathbf{g}_k = \mathrm{vec}(\mathbf{G}_k) \in \mathbb{C}^{MN\times 1}$, the downlink channel from BS to the kth UT can be represented by

$$\mathbf{g}_k^H = \sum_{l=1}^{6} \beta_{l,k} \mathrm{vec}^H(\mathbf{A}(\alpha_{l,k}, \theta_{l,k})) = \boldsymbol{\beta}_k^H \mathbf{C}_k, \tag{28}$$

where $\boldsymbol{\beta}_k = [\beta_{1,k}, \beta_{2,k}, \cdots, \beta_{6,k}]^H$, and

$$\mathbf{C}_k = [\mathrm{vec}(\mathbf{A}(\alpha_{1,k}, \theta_{1,k})), \mathrm{vec}(\mathbf{A}(\alpha_{2,k}, \theta_{2,k})), \cdots, \mathrm{vec}(\mathbf{A}(\alpha_{6,k}, \theta_{6,k}))]^H. \tag{29}$$

With (28), the downlink channel estimation for each UT only needs to estimate 6 unknowns in $\boldsymbol{\beta}_k$. To reuse the overall τ orthogonal training sequences, let us divide K UTs into different groups and clusters. We first gather UTs with different angular signature $\mathcal{B}_k$ that are separated by a certain guard interval into the same group, i.e., $\mathcal{B}_k \cap \mathcal{B}_l = \emptyset$, $\mathcal{B}_k - \mathcal{B}_l \geq \Omega$, $k \neq l$. The same orthogonal training matrix $\mathbf{S}_g = \mathbf{S}_k = [\mathbf{s}_1, \mathbf{s}_2, \cdots, \mathbf{s}_6]^H \in \mathbb{C}^{6\times L}$ can be reused by different UTs in the gth group, where $tr\{\mathbf{S}_k^H \mathbf{S}_k\} = 1$ for $k \in \mathcal{D}_g$ and $\mathcal{D}_g$ is the UT index set of the gth group. Secondly, let us take any $\lfloor \frac{\tau}{6} \rfloor$ groups as a training cluster and define the group index set of the qth training cluster as $\mathcal{D}_q^{tr}$. Different groups in the same training cluster use different 6-traning sequences among all τ training sequence, namely, $\mathbf{S}_{g'} \mathbf{S}_g^H = \mathbf{0}$ for $\mathcal{D}_{g'}, \mathcal{D}_g \in \mathcal{D}_q^{tr}$. Moreover, different training clusters must transmit training sequences in different time slot. For the ease of exposition, assume that all K UTs are divided into G^d groups and G^{dt} training clusters, Namely, $G^{dt} = \lceil G^d / \lfloor \frac{\tau}{6} \rfloor \rceil$.

Let us then take the training of the gth group for example to describe the downlink channel estimation. From antenna array theory, it is easily known that the optimal downlink beamforming vector corresponding to the lth path of the kth UT is $\mathbf{w}_{l,k} = \mathrm{vec}(\mathbf{A}(\alpha_{1,k}, \theta_{1,k}))$ when the number of antennas of BS is infinite.

Then, the overall $MN \times 6$ beamforming matrix that pointing towards the kth UT can be expressed as $\mathbf{W}_k = [\mathbf{w}_{1,k}, \mathbf{w}_{2,k}, \cdots, \mathbf{w}_{6,k}]$, i.e., $\mathbf{W}_k = \mathbf{C}_k^H$. Moreover, the overall beamforming matrix of the gth group is defined as

$$\mathbf{W}_g = \sum_{k\in\mathcal{D}_g} \mathbf{W}_k \Lambda_k, \tag{30}$$

where $\Lambda_k = \mathrm{diag}\{\gamma_{1,k}, \gamma_{2,k}, \cdots, \gamma_{6,k}\}$ is the 6×6 diagonal matrix, and the scalar variable $\gamma_{l,k}$ is the transmit power toward the lth propagation path of the kth UT. Denoting P_k^{dt} as the maximum training power of the kth UT, there is $\mathrm{tr}\{\Lambda_k \Lambda_k^H\} \leq P_k^{dt}$.

Then the received signals at the kth UT in the gth training cluster can be expressed as

$$\begin{aligned} \mathbf{y}_k^H &= \mathbf{g}_k^H \sum_{g\in\mathcal{D}_q^{tr}} \mathbf{W}_g \mathbf{S}_g + \mathbf{n}_k^H \\ &= \boldsymbol{\beta}_k^H \mathbf{C}_k \mathbf{W}_k \Lambda_k \mathbf{S}_k + \sum_{l\in\mathcal{D}_g/\{k\}} \boldsymbol{\beta}_k^H \mathbf{C}_k \mathbf{W}_l \Lambda_l \mathbf{S}_g \\ &\quad + \sum_{g'\in\mathcal{D}_q^{tr}/\{\mathcal{D}_g\}} \boldsymbol{\beta}_k^H \mathbf{C}_k \mathbf{W}_{g'} \mathbf{S}_{g'} + \mathbf{n}_k^H, \end{aligned} \tag{31}$$

where $\mathbf{n}_k^H$ is the noise vector at the kth UT with the elements distributed as $\mathcal{CN}(0, \sigma^2)$.

According to Lemma 3, we can obtain

$$\lim_{M\to\infty, N\to\infty} \mathbf{C}_k \mathbf{W}_l = \begin{cases} \mathbf{I}_k, & k = l \\ \mathbf{0}, & k \neq l, \end{cases} \tag{32}$$

where $\mathbf{I}_k$ is 6×6 identity matrix. Bearing in mind that $\mathcal{B}_k$ and $\mathcal{B}_l$ are separated at least by one guard interval Ω, we know that the second term in (31) approximates to zero for massive URA. Therefore, (31) can be expressed as

$$\mathbf{y}_k^H = \boldsymbol{\beta}_k^H \Lambda_k \mathbf{S}_k + \sum_{g'\in\mathcal{D}_q^{tr}/\{\mathcal{D}_g\}} \boldsymbol{\beta}_k^H \mathbf{C}_k \mathbf{W}_{g'} \mathbf{S}_{g'} + \mathbf{n}_k^H. \tag{33}$$

Since $\mathbf{S}_{g'}\mathbf{S}_k^H = \mathbf{0}$, the complex path gain vector $\boldsymbol{\beta}_k^H$ of UT k can be estimated by the LS method as

$$\hat{\boldsymbol{\beta}}_k^H = \mathbf{y}_k^H(\Lambda_k\mathbf{S}_k)^H((\Lambda_k\mathbf{S}_k)(\Lambda_k\mathbf{S}_k)^H)^{-1} = \boldsymbol{\beta}_k^H + \mathbf{n}_k^H\mathbf{S}_k^H\Lambda_k^{-1}, \tag{34}$$

and there is no interference coming from other UTs in the cluster $\mathcal{D}_g^{tr}$. Hence, the overall estimated channel for the kth UT in the gth group is

$$\hat{\mathbf{g}}_k^H = \hat{\boldsymbol{\beta}}_k^H\mathbf{C}_k = \mathbf{y}_k^H\mathbf{S}_k^H\Lambda_k^{-1}\mathbf{C}_k = \mathbf{g}_k^H + \mathbf{n}_k^H\mathbf{S}_k^H\Lambda_k^{-1}\mathbf{C}_k. \tag{35}$$

Then, each UT only needs to feedback 6 components $\hat{\boldsymbol{\beta}}_k$ to BS such that BS can perform the optimal user scheduling and power allocation for the subsequent downlink data transmission. Compared to the feedback of large amount of measurements in conventional channel estimation method, the overhead of the newly proposed framework is significantly reduced.

The downlink MSE of the LS estimator in (35) can be computed as

$$\mathrm{MSE}_k^d = \mathbb{E}\{\parallel \mathbf{n}_k^H\mathbf{S}_k^H\Lambda_k^{-1}\mathbf{C}_k \parallel^2\} = \sigma_n^2 \parallel \Lambda_k^{-1} \parallel^2 tr\{\mathbf{C}_k^H\mathbf{C}_k\}^{-1}, \tag{36}$$

while the optimal power allocation matrix Λ_k can be obtained from the following problem:

$$\begin{aligned} \min \quad & \sum_{k=1}^{K}\sigma_n^2 \parallel \Lambda_k^{-1} \parallel^2 \ tr\{\mathbf{C}_k^H\mathbf{C}_k\}^{-1} \\ s.t. \quad & \sum_{k=1}^{K} tr\{\Lambda_k^*\Lambda_k\} \le \sum_{k=1}^{K} P_k^{dt}. \end{aligned} \tag{37}$$

Inspecting (37), it can be straightforwardly shown that the matrix Λ_k of the kth UT are the same and there should be $\gamma_{1,k} = \gamma_{2,k} = \cdots = \gamma_{6,k} = \frac{\sqrt{6P_k^{dt}}}{6}$.

It is obvious that the dimension and the complexity of the downlink training has been reduced to a large extent in our newly proposed framework. The sparsity in the angle domain makes it possible to fulfill channel estimation with a small number of pilots, which greatly improves the spectrum efficiency. The user-interference due to pilot reuse will vanish when the angular signatures of the UTs in the same group do not have the same elements. Meanwhile, UTs do not need the knowledge of angular signature set $\mathcal{B}_k$ to perform the estimation of 6 channel parameters $\boldsymbol{\beta}_k$, which is another key advantage of the proposed downlink channel estimation strategy.

B. Downlink Data Transmission With User Scheduling

After obtaining the angular signatures and channel gains of all UTs, we could schedule UTs into different groups to enhence the data transmission efficiency. Meanwhile, the scheduling scheme should maximize the achievable rate for each group under given power constraint.

Assume UTs are scheduled into G^{dd} groups and denote the UT index set of the gth group as $\mathcal{D}_g^{dd}, g = 1, 2, \cdots, G^{dd}$. The received signal y_k over the 6 propagation paths can be expressed as

$$\begin{aligned} y_k &= \mathbf{g}_k^H \sum_{k\in\mathcal{D}_g^{dd}} \mathbf{W}_k\Gamma_k\mathbf{d}_k + n_k \\ &= \boldsymbol{\beta}_k^H\mathbf{C}_k\mathbf{W}_k\Gamma_k\mathbf{d}_k + \sum_{l\in\mathcal{D}_g^{dd}/\{k\}} \boldsymbol{\beta}_k^H\mathbf{C}_k\mathbf{W}_l\Gamma_l\mathbf{d}_l + n_k \\ &= \boldsymbol{\beta}_k^H\boldsymbol{\kappa}_k d_k + n_k = \sum_{l=1}^{6}\beta_{l,k}\kappa_{l,k}d_k + n_k, \end{aligned} \tag{38}$$

where $\boldsymbol{\kappa}_k = [\kappa_{1,k}, \kappa_{2,k}, \cdots \kappa_{6,k}]^H$ denote the normalized power allocation, $\Gamma_k = \mathrm{diag}\{\kappa_{1,k}, \kappa_{2,k}, \cdots \kappa_{6,k}\}$, $\mathbf{d}_k = [d_k, d_k, \cdots, d_k]^H \in \mathbb{C}^{6\times 1}$ is the transmitted signal of the kth UT, and n_k is zero mean circularly symmetric complex Gaussian noise. As seen from (38), the gains of the beams over the 6 propagation paths can be adjusted by controlling the vector $\boldsymbol{\kappa}_k$.

To maximize the achievable rate for each group, UTs in the same group should have non-overlapping angular signatures such that the inter-user interference could be avoided. Thus, we can take a simple method to schedule UTs, where UTs in the same group have non-overlap angular signature, $\mathcal{B}_k \cap \mathcal{B}_l = \emptyset$, $\mathcal{B}_k - \mathcal{B}_l \ge \Omega$ for $k \ne l$. We here try to minimize the number of UT groups while to maximize the sum capacity as much as possible for each time block.

Thus, the throughput of each group can be expressed as

$$R(\mathcal{D}_g^{dd}|P_g) \triangleq \sum_{k\in\mathcal{D}_g}\log_2(1+\rho_k), \tag{39}$$

where P_g is the total power constraint for this group, and ρ_k denotes the data transmission SNR of the kth UT. Moreover, the power constraint is $\sum_{k\in\mathcal{D}_g^{dd}}\rho_k \le P_g$. The optimal power allocation of each group can be simply obtained by the conventional water-filling algorithm [45] to obtain the optimal $\boldsymbol{\kappa}_k$. Obviously, the optimal beam gains should be selected as the estimated channel gains $\boldsymbol{\kappa}_k = \boldsymbol{\beta}_k/\|\boldsymbol{\beta}_k\|$.

With the aforementioned criterion, we provide a greedy user scheduling approach in Algorithm 2. Basically, the UTs with the strongest channel gain will be first scheduled and then the other UTs with non-overlapping angular signatures can join the same group only if the achievable sum-rate of the whole group increases afterwards. Moreover, the power constraint P_g for each group is adjusted dynamically and it is proportional to the final number of UTs in each group.

VI. Simulation Results

In this section, we show the effectiveness of the proposed strategy through numerical examples. The BS is equipped with $M \times N = 100 \times 100$ URA of $d = \lambda/2$, and $K = 30$ active UTs are randomly distributed on the ground and are gathered into 5 spatially distributed clusters. We use the ray-tracing way to model the 60GHz indoor environment channels [46], [47]. The channel matrix of different UTs are formulated according to (2) and (28). The default value of τ is assumed to be $\tau = 12$, and the guard interval for user grouping is set as $\Omega = 4°$. The length of pilot is taken as $L = 12, 24, 36$, respectively.

Algorithm 2 ADMA User Scheduling Algorithm in Downlink Data Transmission

Step 1: Calculate power of estimated channel vector $\| \hat{\mathbf{g}}_k \|^2$ for all UTs.

Step 2: Initialize $g = 1$, $\mathcal{D}_g^{dd} = \emptyset$, $P_g = 0$, $R(\mathcal{D}_g^{dd}|P_g) = 0$, and the remaining UT set $\mathcal{U}_r = \{1, 2, \cdots, K\}$.

Step 3: Select the UT in $\mathcal{U}_r$ with the maximal power of channel, $k = \arg\max_{k \in \mathcal{U}_r} \| \hat{\mathbf{g}}_k \|^2$. Then set $\mathcal{D}_g^{dd} = \mathcal{D}_g^{dd} \cup \{k\}$, $\mathcal{U}_r = \mathcal{U}_r \setminus \{k\}$, $P_g = P_k$, and calculate $R(\mathcal{D}_g|P_g)$ according to (39).

Step 4: Select all UTs in $\mathcal{U}_r$ whose angular signatures are non-overlapping with UTs in $\mathcal{D}_g^{dd}$, and denote them by $\mathcal{D}'_g$, which can be expressed as

$$\mathcal{D}'_g = \{m \in \mathcal{U}_r | \mathcal{B}_m \cap \mathcal{B}_k = \emptyset, \mathcal{B}_k - \mathcal{B}_l \geq \mathbf{\Omega}, \forall k \in \mathcal{D}_g\}.$$

Step 5: If $\mathcal{D}'_g \neq \emptyset$, find a UT k' in $\mathcal{D}'_g$ and set $P'_g = P_g + P_k$, such that

$$k' = \arg \max_{k' \in \mathcal{D}'_g} R(\mathcal{D}_g^{dd} \cup \{k'\}|P'_g).$$

If $R(\mathcal{D}_g^{dd} \cup \{k'\}|P'_g) \geq R(\mathcal{D}_g^{dd}|P_g)$, set $\mathcal{D}_g^{dd} \cup \{k'\}$, $\mathcal{U}_r = \mathcal{U}_r \setminus \{k'\}$, $P_g = P'_g$ and go to **Step 4**.

Step 6: If $\mathcal{U}_r \neq \emptyset$, modify $g = g + 1$, return to **Step 3**.

Step 7: The minimal number of UT group G^{dd} is set as the current g, and the optimal user scheduling result is accordingly given by $\mathcal{D}_1, \mathcal{D}_2, \cdots, \mathcal{D}_{G^{dd}}$.

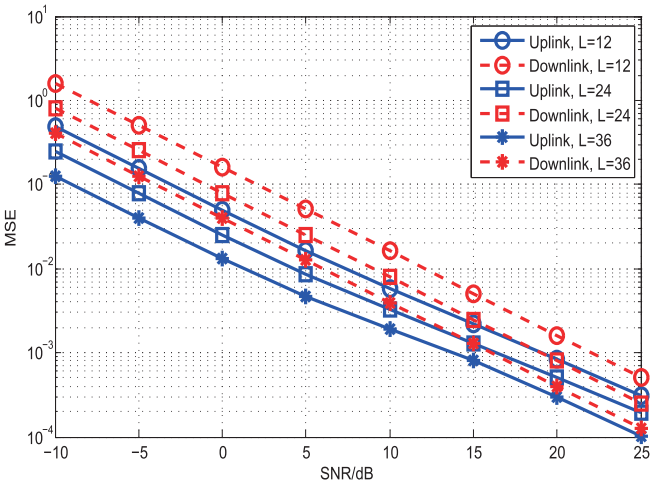

Fig. 7. Comparison of uplink/downlink MSE performances of the proposed channel estimation scheme with $\tau = 12$ and $L = 12, 24, 36$, respectively.

The SNR is defined as $\rho = \sigma_p^2/\sigma_n^2$, and the normalized MSE of the uplink and downlink channels are defined as

$$\text{MSE}_u = \frac{1}{K} \sum_{k=1}^{K} \frac{\| [\mathcal{H}_k]_{(3)} - [\hat{\mathcal{H}}_k]_{(3)} \|^2}{\| [\mathcal{H}_k]_{(3)} \|^2},$$

$$\text{MSE}_d = \frac{1}{K} \sum_{k=1}^{K} \frac{\| \mathbf{g}_k - \hat{\mathbf{g}}_k \|^2}{\| \mathbf{g}_k \|^2}, \quad (40)$$

respectively. In all examples, the angular signatures of all UTs are estimated from the preamble.

Fig. 7 illustrates the MSE performances of uplink/downlink training, respectively, as a function of SNR with different

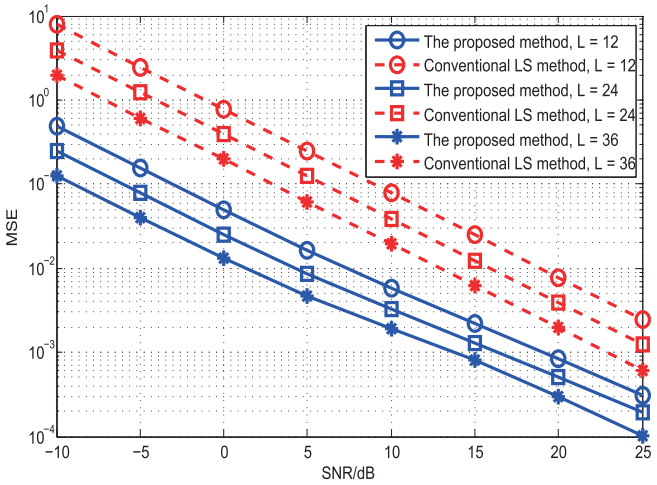

Fig. 8. The uplink MSE performance comparison of the proposed channel estimation method and the conventional LS method, with $\tau = 12$ and $L = 12, 24, 36$, respectively.

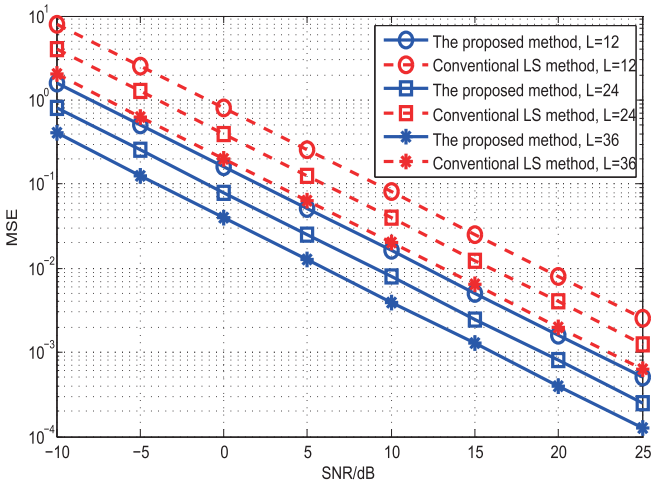

Fig. 9. The downlink MSE performance comparison of the proposed channel estimation method and the conventional LS method, with $\tau = 12$ and $L = 12, 24, 36$, respectively.

training sequence length L. The total power for both uplink and downlink training is constrained to $P_k^u = P_k^d = L \cdot \rho$ for all UTs as a given SNR ρ. For the uplink training, $K = 30$ UTs are divided into $G^u = 12$ groups. All these 12 groups can be scheduled in the same training length L with $\tau = 12$ available orthogonal training sequences. While for the downlink training, $K = 30$ UTs are gathered into 5 groups and are assigned into $G^d = 3$ clusters, i.e., they can be scheduled simultaneously with the limited number of orthogonal training $\tau = 12$ too. It is seen from Fig. 7 that when L increases, the MSE performances of uplink/downlink can be improved, because the total training power is proportional to L. Moreover, it can be seen that the uplink MSE performances are generally better than that of downlink for any SNR and L. This can be inferred by comparing the noise terms of (25) and (36), where the noise power included in the uplink training is only proportional to $\sqrt{L}$ while it is proportional to L for the downlink training.

Fig. 8 and Fig. 9 compare the proposed channel estimation with the convention LS method for both uplink and downlink

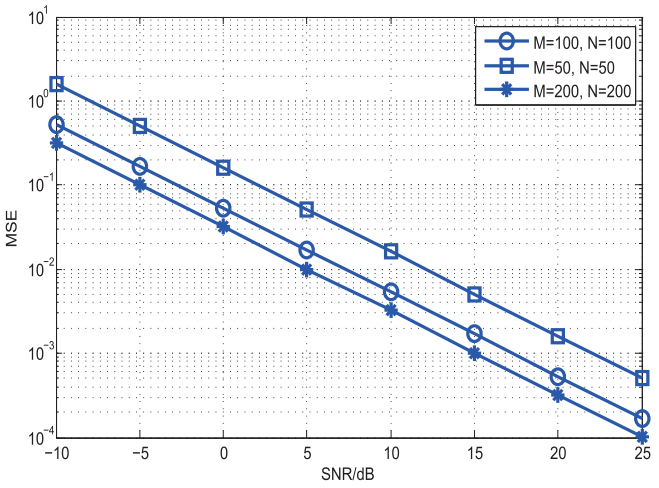

Fig. 10. Comparison of downlink MSE performances with $L = 12$ and $M = 50$, $N = 50$, $M = 100$, $N = 100$, $M = 200$, $N = 200$, respectively.

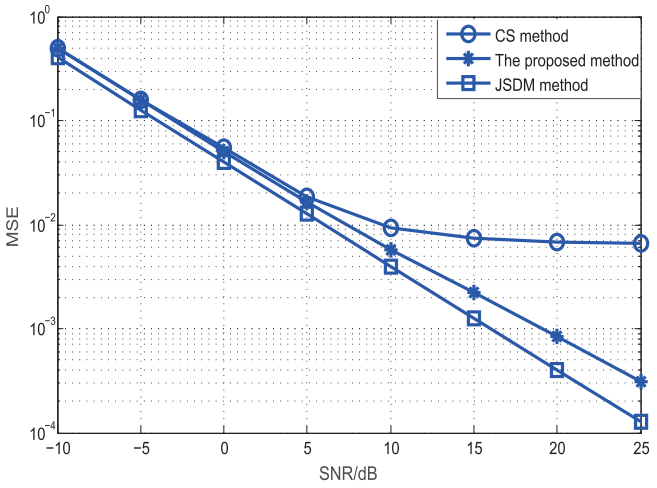

Fig. 11. The downlink MSE performances of the proposed method, JSDM method and the CS-based method

cases. To apply the conventional LS method, $\tau = 30$ orthogonal training sequences are used for uplink case while 10000×10000 orthogonal training matrix is used for downlink case. To be mentioned, the proposed channel estimation method only need $\tau = 12$ orthogonal training sequences after the angle knowledge is obtained from preamble. To provide a fair comparison, the total uplink training power $P_k^u = L \cdot \rho$ is kept the same for any given ρ and L, while the total downlink training power $\sum_{k=1}^{K} P_k^d = KL \cdot \rho$ are kept the same too. It is seen that the proposed channel estimation method performs better than the conventional LS method in any SNR region even when the latter has sufficient number of orthogonal training and when the corresponding computational complexity is affordable. The reasons can be found that the proposed method only involves 6 components of the noise vector while the conventional LS method includes the whole noise power from all antenna elements.

Fig. 10 displays the downlink MSE performances as a function of SNR for different URA sizes. The total power for different number of BS antennas are constrained consistently. It is clearly seen from Fig. 10 that increase the number of BS antennas will improve the channel estimation accuracy for downlink because: (i) increasing the number of BS antennas will improve the angular signatures accuracy; (ii) the second term of (31) is more and more close to zero when the number of BS antennas increases.

Fig. 11 compares the downlink MSE performances of the proposed channel estimation method, the eigen-decomposition based JSDM method [48], and the CS-based method [25]. It can be seen that the MSE performance of JSDM is slightly better than the proposed one, since the former catches the exact eigen-direction to recover the channel. In fact, when the number of antennas in BS is infinite, every steering vector in the proposed method equivalent to the corresponding eigenvector in JSDM method. In this case, the performance of the proposed one is equal to the eigen-decomposition based JSDM method. Nevertheless to obtain the $M \times N$ dimensional channel covariance matrix for JSDM would not

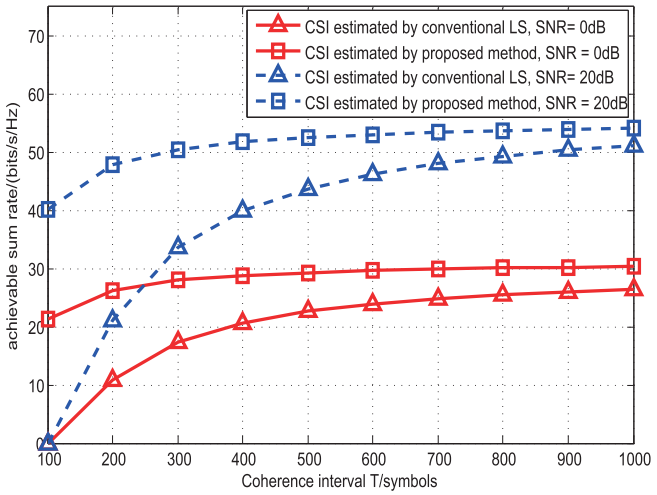

Fig. 12. The average achievable sum rate of the proposed channel estimation method and conventional LS as a function of coherence interval T.

be an easy and stable task in practice. On the other side, the proposed method and CS-based method could directly handle the instantaneous channel estimation but CS-based method has an error floor due to the power leakage problem in it sparse channel representation.

Fig. 12 illustrates the average achievable sum rate for the downlink data transmission, defined as

$$C_{sum} = \left(1 - \frac{T_{pilot}}{T}\right) \sum_{g=1}^{G^{dt}} R(\mathcal{D}_g^{dd} | P_g) / G^{dt}, \qquad (41)$$

where T_{pilot} denotes the length of pilot used for channel training. To make the comparison fair, the overall training power and the overall data power within the coherent time T are set as the same for each method. It can be seen from Fig. 12 that the average achievable sum rate of the proposed method is much higher than that from conventional LS when T is relatively small or when SNR is relatively low. When T becomes large, the training length of LS is small compared to T and then the average achievable sum rate from conventional LS will approach that from the the proposed method.

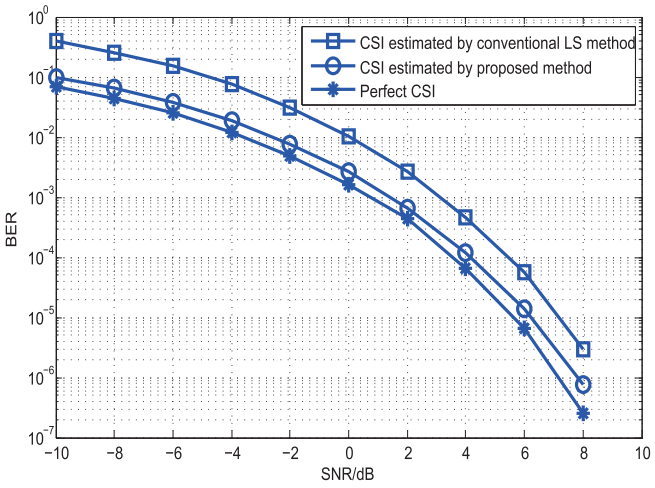

Fig. 13. Comparison of BER performances with perfect CSI, CSI estimated by the proposed channel estimation method, as well as the conventional LS method, respectively, where $L = 12$ and $\tau = 12$.

Lastly, we illustrate the bit error rate (BER) of QPSK modulation for the downlink data transmission in Fig. 13. Three kinds of CSI are compared: perfect CSI, CSI estimated by the proposed method, and CSI from the conventional LS method. To keep the comparison fair, the overall training power is set as the same for each method. It is seen that the BER achieved by the proposed channel estimation method perform better than the conventional LS method by about 1.5dB while possesses less than 1 dB gap from that of the perfect CSI. The results clearly demonstrates the effectiveness of the proposed method.

VII. Conclusion

In this paper, we exploited the antenna array theory for channel estimation 60 GHz indoor massive URA communications environment. We showed that the channel estimation can be decomposed into angular estimation and gain estimation, which is a unique property for massive MIMO systems. We then proposed an array signal processing aided fast DOA estimation algorithm, while the gain information could be obtained with very small amount of training resources, which significantly reduces the training overhead and the feedback cost. Moreover, we utilized the angle reciprocity to facilitate the downlink channel estimation for both TDD and FDD systems. To enhance the spectral and energy efficiency, we also designed an ADMA user scheduling algorithm based on angular information of different UTs. Compared to existing channel estimation algorithms, the newly proposed one does not require any information of channel statistics, can be efficiently deployed by the 2D-FFT operations, and is unified for both TDD and FDD systems, making it a practical solutions for 60 GHz indoor communications.

Appendix
The Introduction of Tensor

An n-mode vector of an $(I_1 \times I_2 \times \cdots \times I_N)$-dimensional tensor $\mathcal{A}$ is an I_N-dimensional vector obtained from $\mathcal{A}$ by varying the index i_n and keep other indices fixed. A matrix unfolding of the tensor $\mathcal{A}$ along the nth mode is denoted by $[\mathcal{A}]_{(n)}$ in which the element $a_{i_1,i_2,\cdots,i_N}$ is at the position with the row number i_n and the column number equal to

$$(i_1-1)I_2\cdots I_{n-1}+(i_2-1)I_3\cdots I_{n-1}+\cdots+i_{n-1}$$
$$(i_{n+1}-1)I_{n+2}\cdots I_N I_1\cdots I_{n-1}+\cdots+(i_N-1)I_1\cdots I_{n-1}.$$

The n-mode product of a tensor $\mathcal{A}\in\mathbb{C}^{I_1\times I_2\times\cdots\times I_N}$ by a matrix $\mathbf{U}\in\mathbb{C}^{J_n\times I_n}$, denoted by $\mathcal{A}\times_n\mathbf{U}$, is an $(I_1\times\cdots\times I_{n-1}\times J_n\times I_{n+1}\times\cdots\times I_N)$-tensor of which the entries are given by

$$(\mathcal{A}\times_n\mathbf{U})_{i_1,\cdots,j_n,i_{n+1},\cdots,i_N}=\sum_{i_n}a_{i_1,\cdots,i_n,i_{n+1},\cdots,i_N}\cdot u_{j_n,i_n}.$$

The outer product of a tensor $\mathcal{A}\in\mathbb{C}^{I_1\times I_2\times\cdots\times I_N}$ and $\mathcal{B}\in\mathbb{C}^{J_1\times J_2\times\cdots\times J_M}$ is given by

$$\mathcal{C}=\mathcal{A}\circ\mathcal{B}\in\mathbb{C}^{I_1\times I_2\times\cdots\times I_N\times J_1\times J_2\times\cdots\times J_M},$$

where $c_{i_1,\cdots,i_N,j_1,\cdots,j_M}=a_{i_1,\cdots,i_N}\cdot b_{j_1,\cdots,j_M}$.

Given the tensor $\mathcal{A}\in\mathbb{C}^{I_1\times\cdots\times I_N}$ and the matrices $\mathbf{F}\in\mathbb{C}^{J_n\times I_n}$, $\mathbf{G}\in\mathbb{C}^{K_n\times J_n}$, and $\mathbf{U}_r\in\mathbb{C}^{J_r\times I_r}$, then we have the following equations

$$\begin{aligned}&(\mathcal{A}\times_n\mathbf{F})\times_n\mathbf{G}\\&\quad=\mathcal{A}\times_n(\mathbf{G}\cdot\mathbf{F})\\&\qquad[\mathcal{A}\times_1\mathbf{U}_1\times_2\cdots\times_R\mathbf{U}_R]_{(r)}\\&\quad=\mathbf{U}_r\cdot[\mathcal{A}]_{(r)}\cdot(\mathbf{U}_{r+1}\otimes\cdots\otimes\mathbf{U}_R\otimes\mathbf{U}_1\otimes\cdots\otimes\mathbf{U}_{r-1}).\end{aligned}$$

The relationship between the tensor and the corresponding matrix multiplication can be expressed as

$$\mathcal{B}=\mathcal{A}\times_n\mathbf{U}_n\Leftrightarrow[\mathcal{B}]_{(n)}=\mathbf{U}_n\cdot[\mathcal{A}]_{(n)}.$$

For example, given a tensor $\mathcal{A}\in\mathbb{C}^{I_1\times I_2\times I_3}$ and the matrices $\mathbf{F}_1\in\mathbb{C}^{J_1\times I_1}$, $\mathbf{F}_2\in\mathbb{C}^{J_2\times I_2}$, and $\mathbf{F}_3\in\mathbb{C}^{J_3\times I_3}$, we have the matrix $[\mathcal{A}]_{(1)}\in\mathbb{C}^{I_1\times(I_2\times I_3)}$, $[\mathcal{A}]_{(2)}\in\mathbb{C}^{I_2\times(I_1\times I_3)}$, and $[\mathcal{A}]_{(3)}\in\mathbb{C}^{I_3\times(I_1\times I_2)}$. Moreover, the 1-mode product of the tensor $\mathcal{A}$ by the matrix $\mathbf{F}_1$ can be expressed as $\mathcal{A}\times_1\mathbf{F}_1\in\mathbb{C}^{J_1\times I_2\times I_3}$, the 2-mode product of the tensor $\mathcal{A}$ by the matrix $\mathbf{F}_2$ can be expressed as $\mathcal{A}\times_2\mathbf{F}_2\in\mathbb{C}^{I_1\times J_2\times I_3}$, and the 3-mode product of the tensor $\mathcal{A}$ by the matrix $\mathbf{F}_3$ can be expressed as $\mathcal{A}\times_3\mathbf{F}_3\in\mathbb{C}^{I_1\times I_2\times J_3}$.

References

[1] C.-X. Wang *et al.*, "Cellular architecture and key technologies for 5G wireless communication networks," *IEEE Commun. Mag.*, vol. 52, no. 2, pp. 122–130, Feb. 2014.
[2] Z. Pi and F. Khan, "An introduction to millimeter-wave mobile broadband systems," *IEEE Commun. Mag.*, vol. 49, no. 6, pp. 101–107, Jun. 2011.
[3] T. S. Rappaport *et al.*, "Millimeter wave mobile communications for 5G cellular: It will work!" *IEEE Access*, vol. 1, pp. 335–349, May 2013.
[4] P. Smulders, "Exploiting the 60 GHz band for local wireless multimedia access: Prospects and future directions," *IEEE Commun. Mag.*, vol. 40, no. 1, pp. 140–147, Jan. 2002.
[5] *60 GHz Band Millimetre Wave Technology*, Radio Frequency Planning Group, Australian Communications Authority, Australia, Dec. 2004.
[6] Z. Ding *et al.*, "Application of non-orthogonal multiple access in LTE and 5G networks," *IEEE Commun. Mag.*, vol. 55, no. 2, pp. 185–191, Feb. 2017.
[7] T. L. Marzetta, "Noncooperative cellular wireless with unlimited numbers of base station antennas," *IEEE Trans. Wireless Commun.*, vol. 9, no. 11, pp. 3590–3600, Nov. 2010.

[8] F. Rusek *et al.*, "Scaling up MIMO: Opportunities and challenges with very large arrays," *IEEE Signal Process. Mag.*, vol. 30, no. 1, pp. 40–60, Jan. 2013.
[9] C. Zhang, Y. Huang, Y. Jing, S. Jin, and L. Yang, "Sum-rate analysis for massive MIMO downlink with joint statistical beamforming and user scheduling," *IEEE Trans. Wireless Commun.*, vol. 16, no. 4, pp. 2181–2194, Jan. 2017.
[10] S. He, C. Qi, Y. Wu, and Y. Huang, "Energy-efficient transceiver design for hybrid sub-array architecture MIMO systems," *IEEE Access*, vol. 4, pp. 9895–9905, Jan. 2017.
[11] Z. Pi and F. Khan, "A millimeter-wave massive MIMO system for next generation mobile broadband," in *Proc. Conf. Rec. 46th Asilomar Conf. Signals, Syst. Comput. (ASILOMAR)*, Nov. 2012, pp. 693–698.
[12] L. You, X. Gao, X. G. Xia, N. Ma, and Y. Peng, "Pilot reuse for massive MIMO transmission over spatially correlated Rayleigh fading channels," *IEEE Trans. Wireless Commun.*, vol. 14, no. 6, pp. 3352–3366, Jun. 2015.
[13] G. Barriac and U. Madhow, "Space-time communication for OFDM with implicit channel feedback," *IEEE Trans. Inf. Theory*, vol. 50, no. 12, pp. 3111–3129, Dec. 2004.
[14] F. Fernandes, A. Ashikhmin, and T. L. Marzetta, "Inter-cell interference in noncooperative TDD large scale antenna systems," *IEEE J. Sel. Areas Commun.*, vol. 31, no. 2, pp. 192–201, Feb. 2013.
[15] R. R. Müller, L. Cottatellucci, and M. Vehkaperä, "Blind pilot decontamination," *IEEE J. Sel. Topics Signal Process.*, vol. 8, no. 5, pp. 773–786, Oct. 2014.
[16] Z. Zhou, J. Fang, L. Yang, H. Li, Z. Chen, and S. Li, "Channel estimation for millimeter-wave multiuser MIMO systems via PARAFAC decomposition," *IEEE Trans. Wireless Commun.*, vol. 15, no. 11, pp. 7501–7516, Nov. 2016.
[17] R. C. de Lamare. (2013)."Massive MIMO systems: Signal processing challenges and future trends." [Online]. Available: https://arxiv.org/abs/1310.7282
[18] S. Le Hong Nguyen and A. Ghrayeb, "Precoding for multicell massive MIMO systems with compressive rank-q channel approximation," in *Proc. IEEE 24th Int. Symp. Pers. Indoor Mobile Radio Commun. (PIMRC)*, Sep. 2013, pp. 1227–1232.
[19] A. J. Duly, T. Kim, D. J. Love, and J. V. Krogmeier, "Closed-loop beam alignment for massive MIMO channel estimation," *IEEE Commun. Lett.*, vol. 18, no. 8, pp. 1439–1442, Aug. 2014.
[20] X. Li, S. Jin, X. Gao, and R. W. Heath, "3D beamforming for large-scale FD-MIMO systems exploiting statistical channel state information," *IEEE Trans. Veh. Technol.*, vol. 65, no. 11, pp. 8992–9005, Nov. 2016.
[21] S. Jin, W. Tan, M. Matthaiou, J. Wang, and K.-K. Wong, "Statistical eigenmode transmission for the MU-MIMO downlink in Rician fading," *IEEE Trans. Wireless Commun.*, vol. 14, no. 12, pp. 6650–6663, Dec. 2015.
[22] C. Sun, X. Q. Gao, S. Jin, M. Matthaiou, Z. Ding, and C. Xiao, "Beam division multiple access transmission for massive MIMO communications," *IEEE Trans. Commun.*, vol. 63, no. 6, pp. 2170–2184, Jun. 2015.
[23] C. Qi, Y. Huang, S. Jin, and L. Wu, "Sparse channel estimation based on compressed sensing for massive MIMO systems," in *Proc. IEEE Int. Conf. Commun. (ICC)*, London, U.K, Jun. 2015, pp. 4558–4563.
[24] Z. Gao, L. Dai, W. Dai, B. Shim, and Z. Wang, "Structured compressive sensing-based spatio-temporal joint channel estimation for FDD massive MIMO," *IEEE Trans. Commun.*, vol. 64, no. 2, pp. 601–617, Feb. 2016.
[25] Z. Gao, L. Dai, Z. Wang, and S. Chen, "Spatially common sparsity based adaptive channel estimation and feedback for FDD massive MIMO," *IEEE Trans. Signal Process.*, vol. 63, no. 23, pp. 6169–6183, Dec. 2015.
[26] A. Maltsev, R. Maslennikov, A. Sevastyanov, A. Lomayev, and A. Khoryaev, "Statistical channel model for 60 GHz WLAN systems in conference room environment," in *Proc. 4th Eur. Conf. Antennas Propag.*, Barcelona, Spain, Apr. 2010, pp. 1–5.
[27] D. Tse and P. Viswanath, *Fundamentals Wireless Communication*. New York, NY, USA: Cambridge Univ. Press, 2005.
[28] O. El Ayach, S. Rajagopal, S. Abu-Surra, Z. Pi, and R. W. Heath, Jr., "Spatially sparse precoding in millimeter wave MIMO systems," *IEEE Trans. Wireless Commun.*, vol. 13, no. 3, pp. 1499–1513, Mar. 2014.
[29] W. Roh *et al.*, "Millimeter-wave beamforming as an enabling technology for 5G cellular communications: Theoretical feasibility and prototype results," *IEEE Commun. Mag.*, vol. 52, no. 2, pp. 106–113, Feb. 2014.
[30] R. O. Schmidt, "Multiple emitter location and signal parameter estimation," *IEEE Trans. Antennas Propag.*, vol. 34, no. 3, pp. 276–280, Mar. 1986.
[31] A. Paulraj, R. Roy, and T. Kailath, "A subspace rotation approach to signal parameter estimation," *Proc. IEEE*, vol. 74, no. 7, 1044–1046, Jul. 1986.
[32] R. Roy, A. Paulraj, and T. Kailath, "ESPRIT—A subspace rotation approach to estimation of parameters of cisoids in noise," *IEEE Trans. Acoust. Speech Signal Process.*, vol. 34, no. 5, pp. 1340–1342, Oct. 1986.
[33] R. Roy and T. Kailath, "Esprit-estimation of signal parameters via rotational invariance techniques," *IEEE Trans. Acoust., Speech, Signal Process.*, vol. 37, no. 7, pp. 984–995, Jul. 1989.
[34] M. Haardt, M. D. Zoltowski, C. P. Mathews, and J. A. Nossek, "2D unitary ESPRIT for efficient 2D parameter estimation," in *Proc. IEEE Int. Conf. Acoust., Speech, Signal Process. (ICASSP)*, Detroit, MI, USA, May 1995, pp. 2096–2099.
[35] L. Cheng, Y.-C. Wu, J. Zhang, and L. Liu, "Subspace identification for DOA estimation in massive/full-dimension MIMO systems: Bad data mitigation and automatic source enumeration," *IEEE Trans. Signal Process.*, vol. 63, no. 22, pp. 5897–5909, Nov. 2015.
[36] A. M. Sayeed, "Deconstructing multiantenna fading channels," *IEEE Trans. Signal Process.*, vol. 50, no. 10, pp. 2563–2579, Oct. 2002.
[37] J. Brady, N. Behdad, and A. M. Sayeed, "Beamspace MIMO for millimeter-wave communications: System architecture, modeling, analysis, and measurements," *IEEE Trans. Antennas Propag.*, vol. 61, no. 7, pp. 3814–3827, Jul. 2013.
[38] A. Alkhateeb, O. El Ayach, G. Leus, and R. W. Heath, Jr., "Channel estimation and hybrid precoding for millimeter wave cellular systems," *IEEE J. Sel. Topics Signal Process.*, vol. 8, no. 5, pp. 831–846, Oct. 2014.
[39] X. Zhang, *Matrix Analysis and Application*, 2th ed. Beijing, China: Tsinghua Univ. Press, 2013.
[40] L. C. Godara, "Application of antenna arrays to mobile communications. II. Beam-forming and direction-of-arrival considerations," *Proc. IEEE*, vol. 85, no. 8, pp. 1195–1245, Aug. 1997.
[41] Recommendations, I. T. U. R, *Propagation Data and Prediction Methods for the Planning of Indoor Radio Communication Systems and Radio Local Area Networks in the Frequency range 900 MHz to 100 GHz*, document I–III, Rec. ITU-R P.1238-7, ITU-R, 2001.
[42] Y. J. Bultitude, and T. Rautiainen, "IST-4-027756 WINNER II D1. 1.2 V1. 2 WINNER II channel models," EBITG, TUI, UOULU, CU/CRC, NOKIA, Tech. Rep., 2007.
[43] *Mobile Wireless Communications Enablers for the Twentytwenty Information Society, EU 7th Framework Programme Project*, document ICT-317669-METIS, METIS, 2013.
[44] R. W. Heath, N. González-Prelcic, S. Rangan, W. Roh, and A. M. Sayeed, "An overview of signal processing techniques for millimeter wave MIMO systems," *IEEE J. Sel. Topic Signal Process.*, vol. 10, no. 3, pp. 436–453, Apr. 2016.
[45] S. P. Boyd and L. Vandenberghe, *Convex Optimization*. Cambridge, U.K.: Cambridge Univ. Press, 2004.
[46] H. Xu, V. Kukshya, and T. S. Rappaport, "Spatial and temporal characteristics of 60-GHz indoor channels," *IEEE J. Sel. Areas Commun.*, vol. 20, no. 3, pp. 620–630, Apr. 2002.
[47] A. Maltsev, R. Maslennikov, A. Sevastyanov, A. Khoryaev, and A. Lomayev, "Experimental investigations of 60 GHz WLAN systems in office environment," *IEEE J. Sel. Areas Commun.*, vol. 27, no. 8, pp. 1488–1499, Oct. 2009.
[48] A. Adhikary, J. Nam, J.-Y. Ahn, and G. Caire, "Joint spatial division and multiplexing—The large-scale array regime," *IEEE Trans. Inf. Theory*, vol. 59, no. 10, pp. 6441–6463, Oct. 2013.

Dian Fan received the B.Eng. degree from the School of Science, Beijing Jiaotong University, Beijing, China, in 2014, where he is currently pursuing the Ph.D. degree with the School of Computer and Information Technology. His research interests include MIMO techniques, massive MIMO systems, millimeter wave systems, and array signal processing.

Feifei Gao (M'09–SM'14) received the B.Eng. degree from Xi'an Jiaotong University, Xi'an, China, in 2002, the M.Sc. degree from McMaster University, Hamilton, ON, Canada, in 2004, and the Ph.D. degree from the National University of Singapore, Singapore, in 2007. He was a Research Fellow with the Institute for Infocomm Research, A*STAR, Singapore, in 2008, and an Assistant Professor with the School of Engineering and Science, Jacobs University, Bremen, Germany, from 2009 to 2010. In 2011, he joined the Department of Automation, Tsinghua University, Beijing, China, where he is currently an Associate Professor.

He has authored/co-authored over 80 refereed IEEE journal papers and over 120 IEEE conference proceeding papers, which have been cited over 3500 times from Google Scholar. His research areas include communication theory, signal processing for communications, array signal processing, and convex optimizations, with particular interests in MIMO techniques, multi-carrier communications, cooperative communication, and cognitive radio networks.

Prof. Gao has served as the technical committee members for many other IEEE conferences. He has served as the symposium Co-Chair of the 2015 IEEE Conference on Communications, the 2014 IEEE Global Communications Conference, and the 2014 IEEE Vehicular Technology Conference. He has served as an Editor of the IEEE TRANSACTIONS ON WIRELESS COMMUNICATIONS, the IEEE COMMUNICATIONS LETTERS, the IEEE SIGNAL PROCESSING LETTERS, the IEEE WIRELESS COMMUNICATIONS LETTERS, the *International Journal on Antennas and Propagations*, and the *China Communications*.

Gongpu Wang received the B.Eng. degree in communication engineering from Anhui University, Hefei, China, in 2001, the M.Sc. degree from the Beijing University of Posts and Telecommunications (BUPT), China, in 2004, and the Ph.D. degree from the University of Alberta, Edmonton, AB, Canada, in 2011. From 2004 to 2007, he was an Assistant Professor with the School of Network Education, BUPT. After graduation, he joined the School of Computer and Information Technology, Beijing Jiaotong University, China, where he is currently an Associate Professor. His research interests include Internet of Things, wireless communication theory, and signal processing technologies.

Zhangdui Zhong received the B.E. and M.S. degrees from Beijing Jiaotong University, Beijing, China, in 1983 and 1988, respectively. He is currently a Professor and an Advisor of Ph.D. candidates with Beijing Jiaotong University, where he is also a Chief Scientist of the State Key Laboratory of Rail Traffic Control and Safety. He is also the Director of the Innovative Research Team, Ministry of Education, Beijing, and a Chief Scientist of the Ministry of Railways, Beijing. His interests include wireless communications for railways, control theory and techniques for railways, and GSM-R systems. His research has been widely used in railway engineering, such as at the Qinghai–Xizang railway, the Datong–Qinhuangdao Heavy Haul railway, and many high-speed railway lines in China. He is an Executive Council Member of the Radio Association of China, Beijing, and a Deputy Director of the Radio Association, Beijing. He has authored or co-authored seven books, five invention patents, and over 200 scientific research papers in his research area. He received the MaoYiSheng Scientific Award of China, the ZhanTianYou Railway Honorary Award of China, and the Top 10 Science/Technology Achievements Award of Chinese Universities.

Arumugam Nallanathan (S'97–M'00–SM'05–F'17) was an Assistant Professor with the Department of Electrical and Computer Engineering, National University of Singapore, from 2000 to 2007. He was with the Department of Informatics, King's College London, from 2007 to 2017, where he was a Professor of Wireless Communications from 2013 to 2017. He has been a Professor of Wireless Communications with the School of Electronic Engineering and Computer Science, Queen Mary University of London, since 2017. He published over 350 technical papers in scientific journals and international conferences. His research interests include 5G wireless networks, Internet of Things, and molecular communications. He was a co-recipient of the Best Paper Award presented at the IEEE International Conference on Communications 2016 and the IEEE International Conference on Ultra-Wideband 2007. He is an IEEE Distinguished Lecturer. He has been selected as a Web of Science (ISI) Highly Cited Researcher in 2016.

Dr. Nallanathan received the IEEE Communications Society SPCE Outstanding Service Award 2012 and the IEEE Communications Society RCC Outstanding Service Award 2014. He served as the Chair for the Signal Processing and Communication Electronics Technical Committee of the IEEE Communications Society, and the Technical Program Chair and a member of Technical Program Committees in numerous IEEE conferences. He was an Editor of the IEEE TRANSACTIONS ON WIRELESS COMMUNICATIONS from 2006 to 2011, the IEEE WIRELESS COMMUNICATIONS LETTERS, and the IEEE SIGNAL PROCESSING LETTERS. He is an Editor of the IEEE TRANSACTIONS ON COMMUNICATIONS and the IEEE TRANSACTIONS ON VEHICULAR TECHNOLOGY.